Dissertation

Reduction of Zinc Oxide Nanoparticles using Microwave In-Liquid Plasma Method

Novriany Amaliyah

2015

Chapter 1

General Introduction

1.1 Problem Statement

The existing energy economy based on fossil fuels reaches a significant risk caused by some aspects, including the raising in the demand for oil, the limitation of non-renewable resources as well as fluctuation of oil prices and the effects of global warming. In the last 30 years, the CO_2 level has almost doubled passing, this result in a rise in global temperature with an associated series of dramatic climate changes[1]. These facts have forced us to consider alternative energy storage and conversion systems, such as the smart grid. In addition, portable electronic equipment and devices have been developing at a fast step, and this progress has demanded ever-increasing energy and power density in power source[2]. Replacement of internal combustion engine (ICE) cars with preferably, zero emission vehicles, i.e. electric vehicles (EVs) or, at least, by

controlling emission vehicles, can solve the CO_2 concern and the consequent air pollution in large urban areas. Figure 1.1 shows estimated CO_2 emissions for battery electric cars and those of conventional petrol and diesel cars. As can be seen, a battery electric car emits less CO_2 than a conventional car.

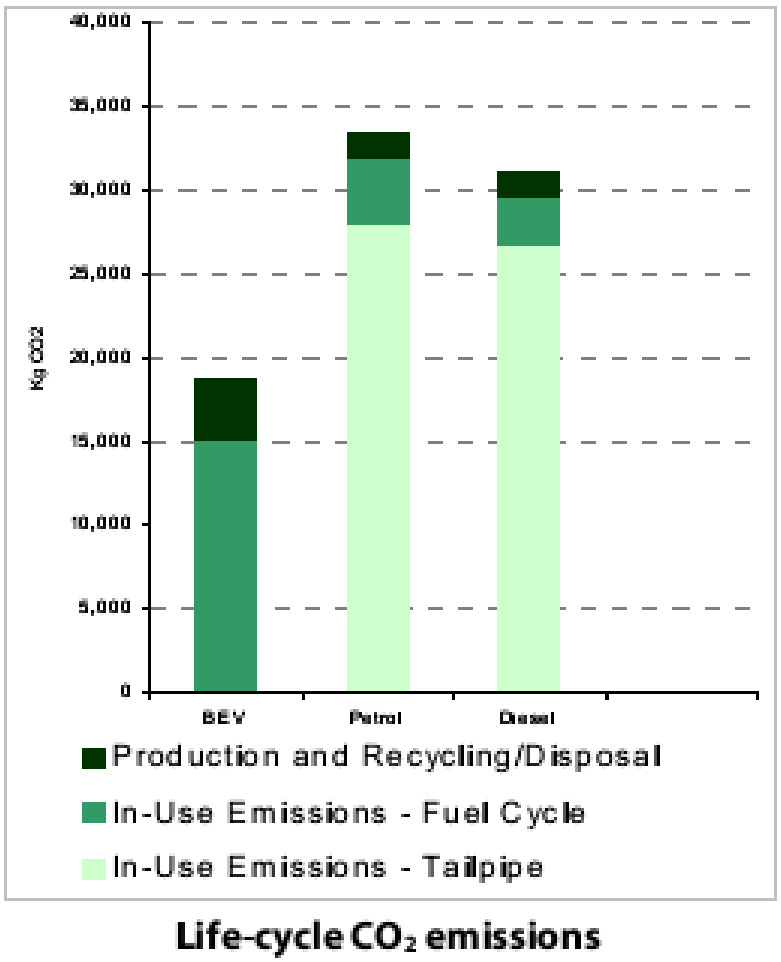

Figure 1.1 Estimated CO_2 emissions arising from the production, disposal,battery electric and conventional petrol and diesel cars.[3]

Electric vehicle batteries are required to cope with high power up to a hundred kilowatt and high-energy capacity up to tens of kilowatt hours within a restricted space and weight. That makes them slightly different from those used consumer electronic device. Recently, the current two major battery technologies commonly used in the electric vehicle are nickel-metal hydride (NiMH) and lithium-ion (Li-ion)[4].

Lithium is the lightest metal elements, and its theoretical energy density is approximately 11,680 h/kg, nearly equivalent to gasoline. In its most conventional structure, a lithium battery contains a graphite anode, a cathode formed by a lithium metal oxide and an electrolyte consisting of a solution of a lithium salt. It is increasingly being thought over to satisfy the demand of energy storage considering that their energy density is higher than that of previous power sources.

However, these batteries are not satisfactory for the practical application of the electric vehicle because of the electrode materials have an intercalation chemistry. Some problems of various natures still prevent the large-scale diffusions of lithium ion batteries for REP and EV application[1]. This makes the current lithium-ion batteries have a limited maximum energy density.

Beside that, safety has also become a serious problem in lithium ion battery technology. The major hazard offered by lithium-ion battery technologies is the evolution of a fire, as a result of the flammability of the substances used in the battery. Consequently, many approaches are under study with the aim to reduce safety hazard[5].

Therefore, metal-air batteries have attracted much attention as a possible alternative, because their energy density is extremely high compared to that of other rechargeable batteries[2]. In metal-air batteries, the cathode reaction is reduction of oxygen and have the highest energy density since the cathode active material is not stored in the battery and is drawn from the ambient air[6]. This theoretically simplifies the design and these batteries are also referred to as fuel cell or battery hybrids.

Metal-air batteries have the potential to store more energy than lithium-ion batteries, which are now used in electric vehicles and some grid applications. Based on the materials used, metal-air batteries could also be less expensive than lead-acid batteries, the cheapest, widely used rechargeable batteries. Table 1 and figure 1.3 shows a comparison between zinc-air and lithium-air batteries.

Table 1.1 Comparison between zinc-air and lithium-air batteries

Zinc-air	Lithium-air
Stable at contact with water	Instability with water, increases manufacturing cost
Cheap raw materials	High cost of lithium and no aqueous electrolytes
Known technology (primary), already exist some companies with systems near realization	At stage of fundamental research
Bad reversibility of Zn electrode, high over potentials at air electrode	Good reversibility
Low voltage of cell	High voltage of cell
1300 Wh/kg	Up to 11000 Wh/kg

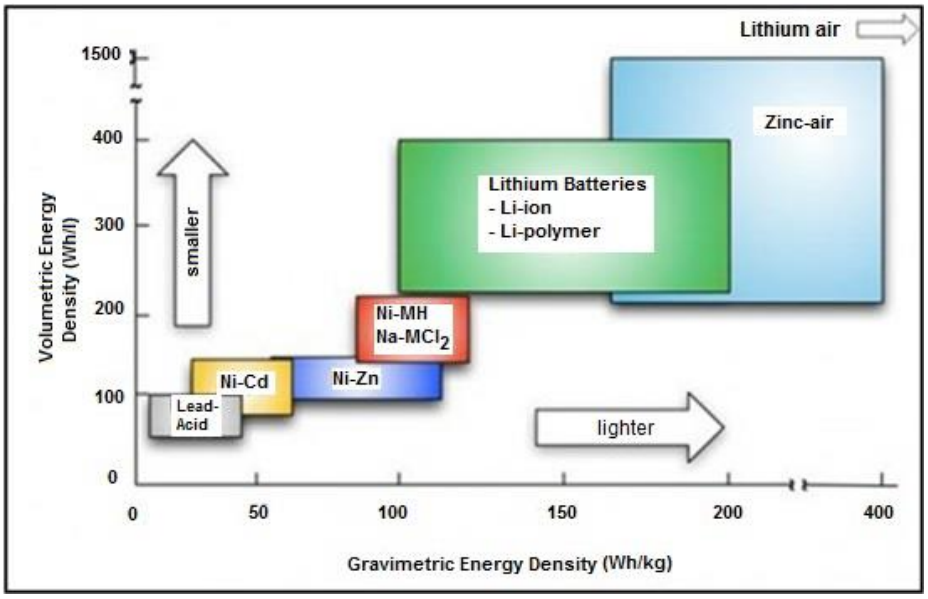

Figure 1.2 The gravimetric energy densities for various types of rechargeable batteries (Source : Revolt Technology)

Although such batteries are commercially successful, they are reaching the limits in performance using the current electrode and electrolyte materials. Application for nanomaterial devices become a breakthrough in material for new generations of batteries, not only for applications in consumer electronics, but especially for clean energy storage and use in hybrid electric vehicles.[8]

Recently, nanostructured materials have also attracted attention for application in energy storage devices, especially for those with high charge/discharge current rates such as batteries. The development of next-generation energy storage devices with high power and high-energy density is a key to the prosperity of electric and hybrid-electric vehicles (EVs and HEVs, respectively), which are expected to at least gradually replace conventional vehicles and help figure out the problems of air pollution and climate change.

In the field of energy storage, the nanotechnological market potential concern first and foremost, enhanced batteries for portable electronics or hybrid and electric vehicles, nano-optimized supercapacitors and nonporous hydrogen storage material. The world market for battery materials showed a double-digit growth rate and amounts to more than 1.2 billion dollars[9].

Market potentials of nanotechnology in the energy conversion sector will mainly arise in the field of thin layer solar cells and in the fuel cell technology. According to estimates by scientific as shown in figure 1.3, a market volume of approximately 10 billion dollars will be reached these applications.

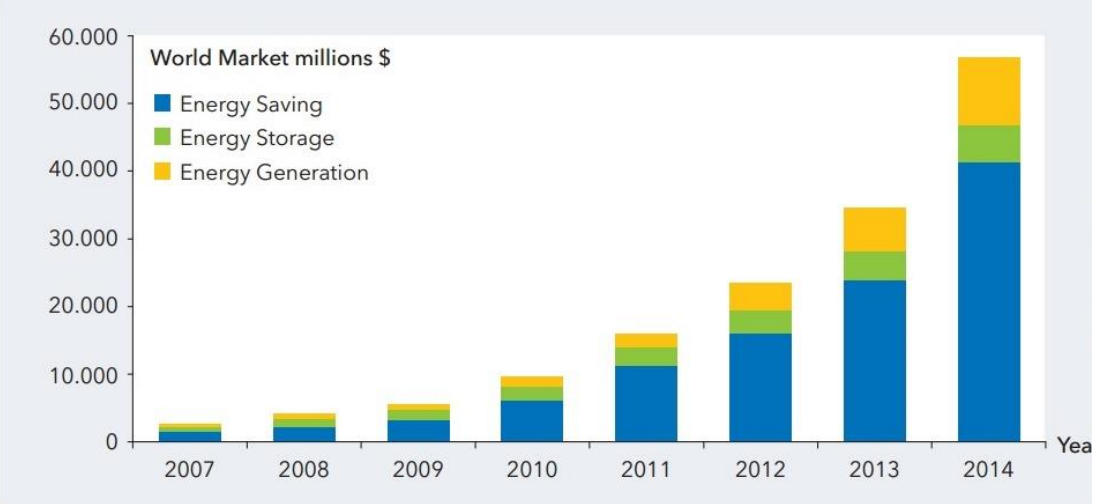

Figure 1.3 World market evaluation for nanotechnology applications in the energy sector (source : Cientifica 2007)

From materials point of view, significant improvements in the areas of battery cathodes, anodes, electrolytes, and separators are needed in order to meet the required energy density, rate capability and the operating temperature range. It is expected that the use of nanomaterial-based anodes and cathodes will be

required to meet the requirements of the batteries used in the next generation HEVs and PHEVs.

Energy density is a function of the amount of battery material which can be packed into a given volume and surface. Traditionally, battery material particle size has been measured in microns. However, by producing the same materials on a nano scale, the packing density of material can be improved and hence the energy density. This approach also improves surface area.

In lithium-ion batteries, nanocrystalline intermetallic alloys, nanosized composite materials, carbon nanotubes, and nanosized transition-metal oxides show higher capacity and better cycle life as cathode materials than their usual larger-particle equivalents. The addition of nanosized metal-oxide powders to polymer electrolyte improves the performance of the polymer electrolyte for all solid-state lithium rechargeable batteries.[10][11]

Among the various metal–air batteries, the zinc–air battery has been thought over as an attractive choice considering of its unique benefits, such as low cost, safety, and environmental benignity[12]. The only metal-air battery systems available worldwide are primary zinc-air batteries. Rather than alkaline batteries, the specific energy of these batteries is 400-450 Wh/kg, which is five

times higher and twice as high as primary lithium battery[13]. However, there are a number of potential problems with these cathode compartments such as mechanical breakdown generated on the catalyst from the air–cathode surface caused by oxygen evolution during charging, atmospheric CO_2 can react with hydroxyl ions to form carbonates, formation of discharge product ZnO deposit on the surface can lead to severe failure of the air cathode, which will limit the lifetime of a zinc–air battery with a large over potential.

Zinc-air batteries generate electricity by combining atmospheric air with zinc metal in a liquid alkaline electrolyte with a resulting byproduct of zinc oxide. When the battery is recharged, the zinc oxide turns back into its constituent parts: oxygen and zinc metal. The large quantities formation of zinc oxide requires a method of recycling the air batteries because it is necessary to balance zinc production and its recycling in order to prevent from decreasing energy use and minimizing emission as well as reducing waste materials.

Plasma in-liquid method has been successfully in synthesis some metal nanoparticles such as zinc[14], zinc oxide[15], magnesium[15], tungsten[16], and silver[15] using a microwave generator and high frequency. This method also provides oxidation and reduction condition based on the solvent used and

prevention from re-oxidation because the reaction area is separated from the air by the liquid.

From a commercial point of view, this is a very important area of study for the development in a rechargeable zinc–air battery under practical conditions.

1.2 Purpose and Construction of Study

The purpose of this study is the application of plasma in-liquid method for oxide reduction of zinc oxide in order to produce zinc nanoparticle. The in-liquid plasma method has been successful to synthesis many kinds of metal nanoparticles including zinc and zinc oxide. The technology for synthesizing zinc or zinc oxide nanoparticles has been published in many papers. However, few papers focusing on reducing zinc oxide become zinc nanoparticles.

The ultimate goal of this research is to reduce oxide in zinc oxide for the purpose of recycling zinc nanoparticles for zinc air battery, which zinc oxide itself is the product of battery as a waste. The studies were proceeded in following procedures and method.

To achieve the aim discussed in the previous section, chapter 2 begins with a description of the definition of nanotechnology. In this chapter, brief

descriptions of the metal nanoparticles and various method for producing metal nanoparticles are also discussed. Plasma in-liquid method of synthesis of metal nanoparticles is examined, with a description of mechanism of plasma discharges in liquid and microwave application.

Synthesis and characterization of material for metal air battery are examined in chapter 3. Application of nanotechnology in metal air battery is also presented in this chapter. In this chapter, brief discussions of zinc nanoparticle for air battery are presented, including working principle of zinc air battery and its application in the electric vehicle.

In chapter 4, microwave plasma in-liquid with ethanol as a reduction agent, is used for reduction of zinc oxide and synthesis zinc nanoparticles. The synthesized materials were identified using an absorption spectrophotometer, energy dispersive x-ray spectrometry, x-ray diffraction and transmission electron microscope. The reduction was confirmed from the absorption spectroscopy result. ZnO peak was decreased in the observed wavelength, that based on Beer-Lambert Law predicted that the intensity of an absorption peak is directly proportional to the concentration of the compound.

The influence of alcoholic solvent at high input power of microwave generators used for the reduction of oxides is presented in chapter 5. Methanol and ethanol were used as a reducing agents. Chemical potential calculation of ethanol and methanol were determined to predict the chemical equilibrium. Theoretical analysis of thermal equilibrium confirmed that in order to reduce oxide, the appropriate temperature by in-liquid plasma method is found to be in the range of 1500 to 2000 K. From the mole fraction of thermal equilibrium, enthalpy needed for reduction using ethanol and methanol was compared. In addition, emission spectrum was conducted and nanoparticles shaped investigated using transmission electron microscope.

The results of studies are summed up in chapter 6.

References

[1] B. Scrosati and J. Garche, "Lithium batteries: Status, prospects and future," *Journal of Power Sources*, vol. 195, no. 9, pp. 2419–2430, May 2010.

[2] J.-S. Lee, S. Tai Kim, R. Cao, N.-S. Choi, M. Liu, K. T. Lee, and J. Cho, "Metal–Air Batteries with High Energy Density: Li–Air versus Zn–Air," *Advanced Energy Materials*, vol. 1, no. 1, pp. 34–50, Jan. 2011.

[3] A. E. & Environment, "Hybrid Electric and Battery Electric Vehicles," *Suistainable Energy Ireland*, vol. November, 2007.

[4] Y. Yang, Y. I. Cho, and A. Fridman, *Plasma Discharge in Liquid*. Taylor & Francis Group, 2012.

[5] "Safety of lithium-ion batteries," 2013.

[6] M. Balaish, A. Kraytsberg, and Y. Ein-Eli, "A critical review on lithium–air battery electrolytes.," *Physical chemistry chemical physics : PCCP*, vol. 16, no. 7, pp. 2801–22, Feb. 2014.

[7] Revolt Technology Presentation, "Rechargeable Zinc-Air Batteries."

[8] M. C. dos Santos, O. Kesler, and A. L. M. Reddy, "Nanomaterials for Energy Conversion and Storage," *Journal of Nanomaterials*, vol. 2012, pp. 1–2, 2012.

[9] W. Luther, "Application of Nano- technologies in the Energy Sector," 2008.

[10] J. Wang, Y. Li, and X. Sun, "Challenges and opportunities of nanostructured materials for aprotic rechargeable lithium–air batteries," *Nano Energy*, vol. 2, no. 4, pp. 443–467, Jul. 2013.

[11] C. Jiang, E. Hosono, and H. Zhou, "Nanomaterials for Nanostructured materials are currently of interest for lithium ion," vol. 1, no. 4, 2006.

[12] Y. Xu, X. Xu, G. Li, Z. Zhang, G. Hu, and Y. Zheng, "Experimental Research of Liquid Infiltration and Leakage in Zinc Air Battery," *Int. J. Electrochem. Sci*, vol. 8, pp. 11805–11813, 2013.

[13] M. Bergman, "Synthesis, preparation and characterisation of materials for metal air battery applications," *Master Thesis, Chalmers University of Technology, Sweden*, 2013.

[14] Y. Hattori, S. Mukasa, H. Toyota, T. Inoue, and S. Nomura, "Synthesis of zinc and zinc oxide nanoparticles from zinc electrode using plasma in liquid," *Materials Letters*, vol. 65, no. 2, pp. 188–190, Jan. 2011.

[15] Y. Hattori, S. Mukasa, H. Toyota, T. Inoue, and S. Nomura, "Continuous synthesis of magnesium-hydroxide, zinc-oxide, and silver nanoparticles by microwave plasma in water," *Materials Chemistry and Physics*, vol. 131, no. 1–2, pp. 425–430, Dec. 2011.

[16] Y. Hattori, S. Nomura, S. Mukasa, H. Toyota, T. Inoue, and T. Usui, "Synthesis of tungsten oxide, silver, and gold nanoparticles by radio frequency plasma in water," *Journal of Alloys and Compounds*, vol. 578, pp. 148–152, Nov. 2013.

Chapter 2

Synthesis of Metal Nanoparticle

2.1 Introduction

Nanotechnology is defined with matter at the scale of 1 billionth of a meter (i.e., 10 − 9 m = 1 nm), and is also examined about manipulating matter at the atomic and molecular scale. A nanoparticle is the most fundamental component in the fabrication of a nanostructure, and is far smaller than the world of everyday objects that are described by Newton ' s laws of motion, but bigger than an atom or a simple molecule that is governed by quantum mechanics.

The prefix “nano” is derived from the Greek word for dwarf. A human hair is approximately 80,000 nm wide, and a red blood cell approximately 7000 nm wide. Figure 2.1 shows the nanometer in context[1]

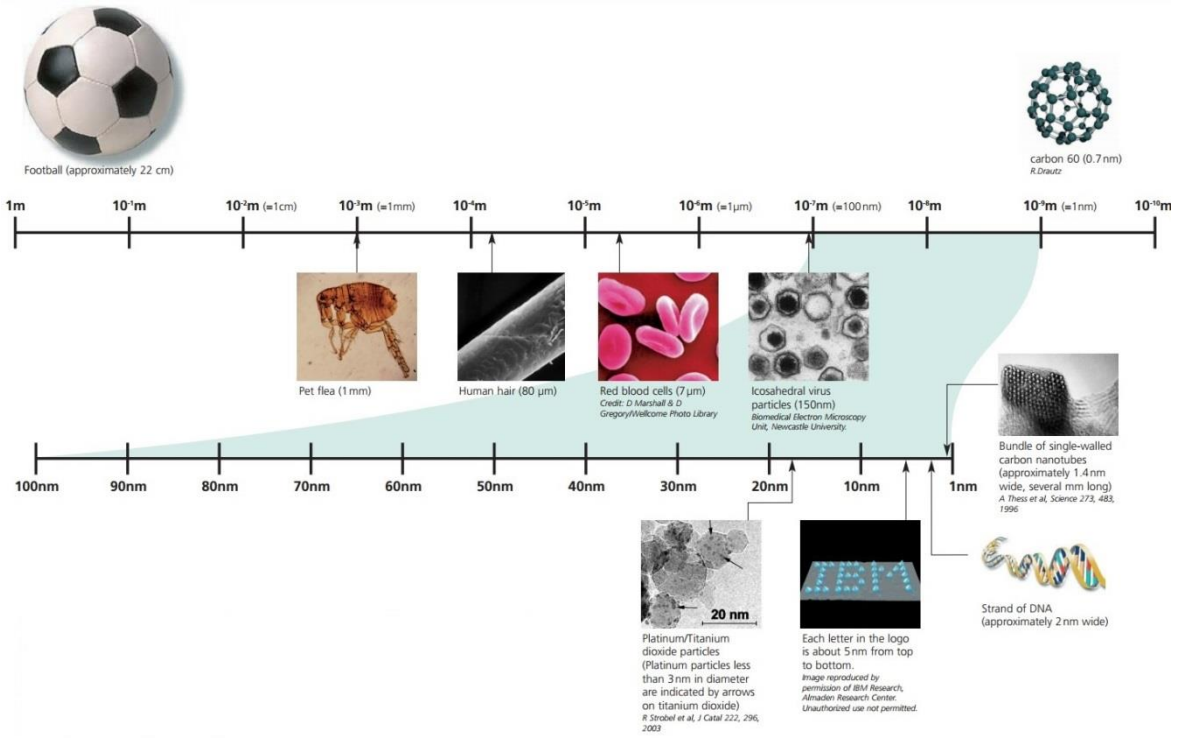

Figure 2.1. Length scale showing nanometer in context (Source : Nanoscience and Nanotechnologies : oppurtunities and uncertainties, 2004)

Nanostructuring in general obtains significantly higher chemical reactivity, as materials broken down to nanoscale substructure show a strongly increased ratio of reactive surface atoms to inert particles in solid. In a particle with a diameter of 20 nm, for example, approximately 10% of the atoms are on the surface, while in a particle of 1 nm the ratio of reactive surface atom amount to already 99%. Figure 2.2 shows that the smaller the particle, the larger the portion of particles presents on the reactive surface of the particles (blue) in contrast to the more inert center of the particle (red). With particle sizes between 1 nm and 20 nm, the ration of surface particle to the total number of particles varies considerably[2].

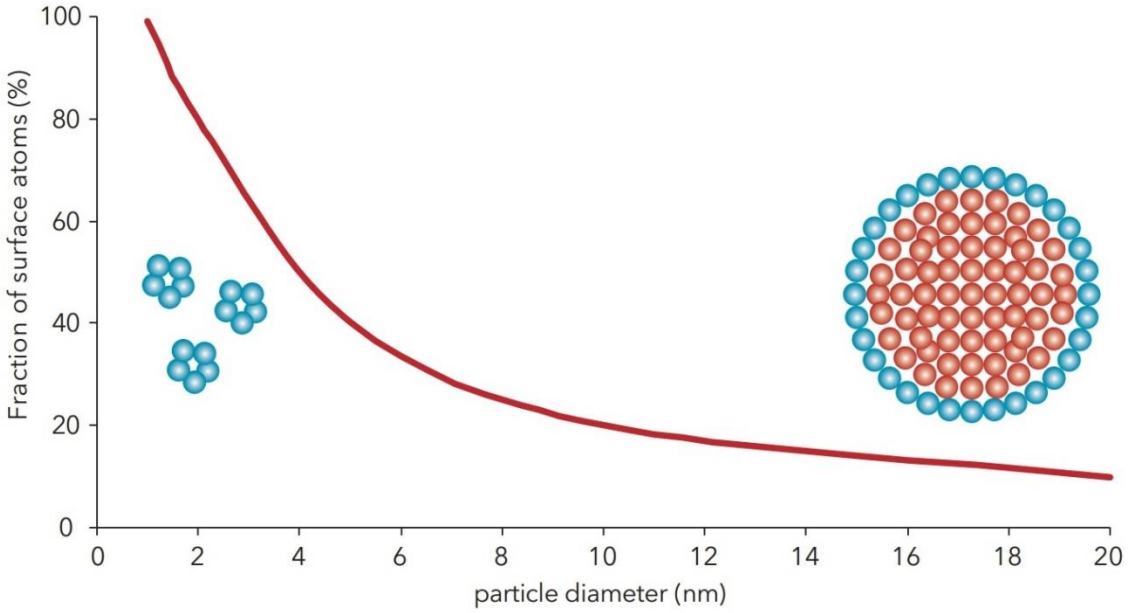

Figure 2.2 The ratio of surface particles to particle diameter (Source : W.Luther, Application of nano-technologies in the energy sector, 2008)

Metallic nanoparticles have unusual physical and chemical properties from bulk metals (e.g., lower melting points, higher specific surface areas, specific optical properties, mechanical strengths, and specific magnetizations), properties that might prove attractive in various industrial applications. It has some main characteristics such as, large surface area to volume ratio as compared to the bulk equivalents, large surface energies, plasmon excitation, quantum confinement, and short range ordering.

Electron delocalization within the bulk matrix in the bulk metal results generally ductile and possess high thermal and electrical conductivity. In contrast, such physical properties are not typically among metal nanoparticles, as the delocalisation observed in the bulk is normally absent, thus giving rise to properties that are totally different to those of the bulk equivalent. Compare to the bulk equivalent, metal nanoparticles have a large surface-area-to-volume ratio. The electrons in nanoparticles are confined to spaces that can be as small as few atom's width across, giving rise to the quantum size effect. These properties make them become particularly interesting candidates for catalytic applications. In addition to these unique properties, the synthesis of metal nanoparticles also provides control on the size and surface composition of particles.[3]

In 1857, Faraday became the first recognized the existence of metallic nanoparticles in solution and in 1908 continued by Mie, who explained the quantitative of their colors. However, how a nanoparticle is viewed and is defined depends very much on the specific application. In this regard, Table 2.1 summarizes the definition of nanoparticles and nanomaterials by various organizations.[4]

Table 2.1 Definitions of nanoparticles and nanomaterials by various organizations

	Nanoparticle	Nanomaterial
ISO	A particle spanning 1-100 nm (diameter)	-
ASTM	An ultrafine particle whose length in 2 or 3 places is 1-100 nm	-
NIOSH	A particle with diameter between 1 and 100 nm, or a fiber spanning the range 1-100 nm	-
SCCP	At least one side is the nanoscale range	Material for which at least one side or internal structure in the nanoscale
BSI	All the fields or diameters are in the nanoscale range	Material for which at least one side or internal structure is in the nanoscale
BAuA	All the fields or diameters are in the nanoscale range	Material consisting of a nanostructure or a nanosubstance

ISO : International Organization for Standarization
ASTM : American Society of Testing and Materials
NIOSH : National Institute of Occupational Safety and Health
SCCP : Scientific Committee on Consumer Products
BSI : British Standards Intitution
BAuA : Bundesanstalt fur Arbeitsschutz und Arbeitsmedizin

Nanoparticles are not necessarily produced by modern synthesis laboratories, but have obviously existed in nature for a long time, and therefore, their use can be traced back to ancient times. While the application of clay minerals as natural nanomaterials does not seem to be very sophisticated, the controlled reinforcement of a ceramic matrix with natural asbestos nanofibers more than 4500 years ago is more intriguing. However, the most spectacular effects were obtained with metal nanoparticles as color pigments in luster and glass technology. Metallic cluster decorations of glazed ceramics appeared in Mesopotamia during the 9^{th} century. [5]

Ideally, metal nanoparticle should be prepared by a method which is reproducible, easy and cheap. It also may control the shape of the particles, use a reaction temperature close to room temperature with a few synthetic steps as possible and could minimize the quantities of generating by-products and waste.[6]

Metal nanoparticles have already been found in a wide variety of fields in many fascinating applications, including conductors, chemical sensors, biosensors,

photovoltaic devices, drug delivery, fuel cells, light-emitting diodes, industrial lithography, quantum dots, quantum wires, quantum devices, air battery, and catalysis.[3]

2.2 Metal Nanoparticle synthesis

There are two fundamental strategies used to prepare the metal nanoparticles: bottom-up and top-down. The bottom up approach is a basic technique to prepare the metal nanoparticles by reducing their ions and the growth of nanoparticles is usually stopped by an agent such as a surfactant or stabilizer. Bottom-up technique includes chemical reduction, electrochemical reduction and thermal method. This technique allows large-scale synthesis of nanoparticles. [7]

Various preparation techniques for nanoparticles (nanomaterials) are summarized in Figure 2.3[4]

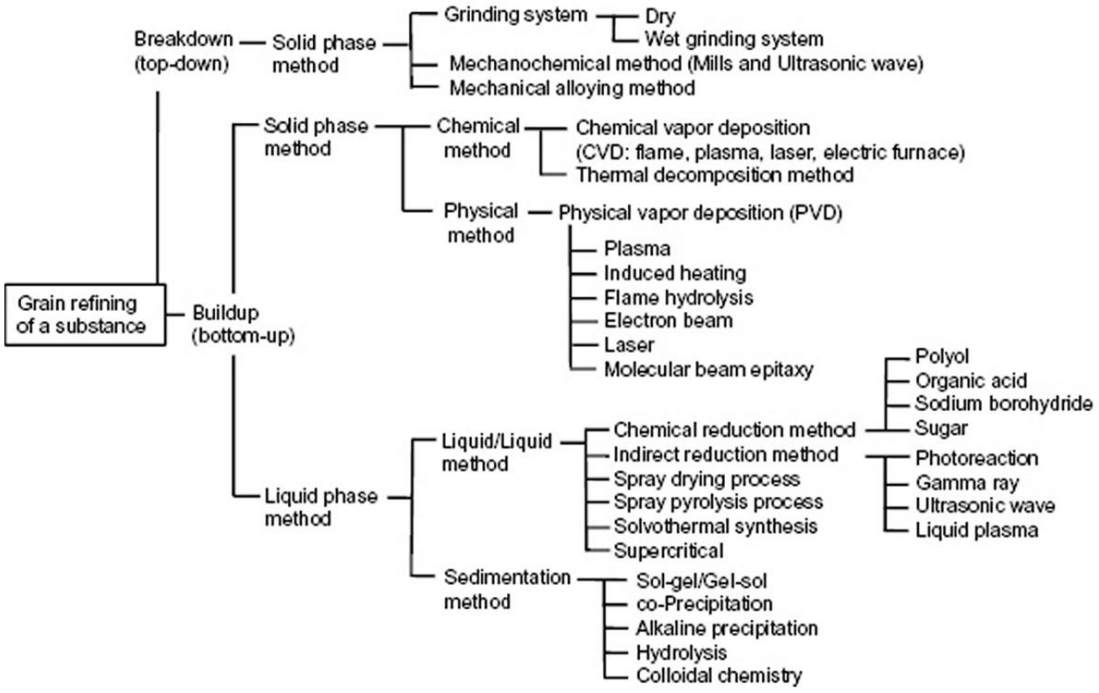

Figure 2.3. Typical synthetic methods for nanoparticles for the top-down and bottom-up approaches

(Source : Microwave in nanoparticle synthesis, John Wiley & Sons 2013)

Due to technological and economic reason, the top-down approach could not achieve the production of structures with infinitesimal dimensions. In contrast, the bottom-up method which based on chemistry can produce a diverse range of nanostructures at relative low cost, with high through output and the potential for large-scale industrial production. Since bottom-up processes are driven mainly by the reduction of Gibbs-free energy, the as-formed nanostructures are in a state

closer to the thermodynamic equilibrium state. In comparison with top-down methods, therefore, bottom-up approached based on chemistry promise a better chance to design, fabricate, and manipulate nanostructure with fewer defect, and more homogenous chemical compound[4].

Throughout a simple reduction of metal ions in the presence of some additive reagents, some metal nanoparticles (palladium and gold) can be synthesized[8]. Green synthesis of noble metal (Au, Ag, Pt) nanoparticles, assisted by plant-extract were reported by Sanches et.al.[9], Kulkarni et.al[10], and Makarov et.al[11]. Laser induced of silver nanoparticles formed by laser ablation technique in acetone was studied by Tarasenko et.al.[12]. Microwave assisted synthesis of metallic nanostructure in solution have been applied in synthesis of Ag, Au, Pt, and AuPd nanostructures[13], while in gas phase iron (Fe) and nickels (Ni) were prepared in a direct current microplasma reactor[14]. Plasma in-liquid using high frequency and microwave generator have been synthezised zinc[15], zinc oxide[16], silver and gold[17], tungsten trioxide[18] nanoparticles from metallic rod.

By applying chemical method, palladium and platinum nanoparticle were synthesized using colloid chemistry[19]. Chemical methods involving the polyol process allowed to get either isotropic or insotropic gold and silver nanoparticles[20].

Various techniques to prepare metal nanoparticles of controlled shape, dimension and orientation have been reported, allowing numerous nanostructures to be readily obtained. Extensive research has been carried out on noble metal nanoparticles, some of which have found application in recent years. However, it is difficult to control the morphology of many base metal nanostructure because they are easily oxidized. Once environmentally friendly, inexpensive methods to prepare base metal nanostructures, including those of base metals, are established, it is estimated that the application of metal nanostructures will spread out significantly[21].

2.3 Plasma in-liquid method for metal nanoparticle synthesis

Plasma is often referred to as the fourth state of matter in which a certain portion of particles in gas or liquid is ionized. The ionization of the neutral particles

is usually achieved through heating. Molecules become energetic and transform in sequence from solid to solid, gas, and a plasma state as temperature rises. In the plasma state, freely moving particles, including electrons and positively or negatively charged ions, make them electrically conductive and can reach electrical conductivities sometimes larger than metal such as gold and copper[22].

For many years, liquid phase methods have been the major preparation method of nanoparticles. Although vapor-phase synthesis methods can produce large quantity of nanoparticles, agglomeration and non-uniform in particle size and shapes are typical problems, especially for nanoparticles on the smaller end of the nanometer range. Liquid-phase method can be sub-divided into liquid/liquid methods, and sedimentation method. Chemical reduction of metal ions is a typical sample of a liquid/liquid method. With this method, it is possible to fine-tune the shape and size of the nanoparticles by changing the reduction agent, the dispersing agent, the reaction time and temperature. Another reduction method, such as photoreduction applying gamma rays, ultrasonic waves, and liquid plasma can be used to prepare nanoparticles. These methods that do not use a chemical reducing

substance have the attractive features that no extraneous impurities are added to the nanoparticles. Other than these methods, sprays drying, spray pyrolysis, solvothermal synthesis, and the supercritical method are also known.

There is no general model that describes the nucleation of particles of various materials in plasma, because the underlying chemistries are different for each material.

2.3.1 Mechanisms of Plasma Discharges in Liquids

Interest has increased recently in plasma discharge in liquids because of the promising applications for various biological, medical, and environmental technologies.

In the liquid, especially water, there are two mechanisms of plasma discharges and breakdowns. The first considers that the breakdown in water as a sequence within the bubbles, while the second group divides the process into partial discharge and a fully developed discharge, such as arc or spark. Based on first approach, the bubble process starts from a microbubble formed by the vaporization of liquid from local heating in the strong electric field region at the tip of the

electrode. From the second approach, the discharge process is divided into partial electrical discharges and arc or spark discharge. In the partial discharges, the current is mostly transferred by ions while in the arc or spark discharge, the current is transferred by electrons. The high current heats a small volume of plasma in the gap between the two electrodes, generating a quasithermal plasma. High current discharge takes place between two submerged electrodes in a high voltage. At this condition a large part of the energy is consumed in the formation of a thermal plasma channel. This channel emits UV radiation, and its expansion against the surrounding water generates intense shock wave[23]. The plasma layer due to the heating of the solution is generated at the interface between the electrode and the solution when a high direct current (DC) voltage is applied.

2.3.2 Plasma for Nanomaterial Processing

In order to modify the property of materials, chemical reactive plasma discharge is extensively used. Plasma processing is a well-established technology that is essential to material manufacturing in numerous industries, including electronics, textiles, automobile, aerospace, and biomedical. Plasma technology also

offers several advantages for nanomaterial processing. Low temperature plasma allows chemical processes to be performed near room temperature, an important consideration to lower costs and make processing compatible with device manufacturing. In addition, plasma-based processing is scalable because materials are usually prepared continuously or over large areas. Perhaps the most important driving force for using plasma technology is chemical purity that is unmatched by any other chemical process and the reason why plasmas have been essential to microelectronic device fabrication[25].

In the solution method of producing nanoparticles mostly requires a simple experimental setup. It is also no need to supply any gas and can be applied to any electrically conductive metal/alloy[24].

A complex plasma contains a wealth of reactive species that can interact with each other to produce either functional nanoassemblies or undersired material.

Zinc, zinc-oxide, magnesium-hydroxide, and silver nanoparticles are synthesized from metallic rod electrode by plasma in-liquid generated by microwave. These nanoparticles are continuously synthesized by manually feeding

a target rod in water and alcohol[15], [16]. By using radio-frequency plasma in liquid, tungsten-oxide, silver, and gold nanoparticles were produced in the developed system[17].

For the in-liquid synthesis, generally nanoparticles are produced at high temperatures induced by plasma to enhance chemical reactivity and then quickly contact the liquid to cool rapidly.

The fullerene C_{60} and titanium oxide nanopowder were synthesized by electric discharge by using pulsed plasma in liquid. This method did not need vacuum system, cooling system and in addition to the low electrical power[26].

Dual plasma electrolysis, which consist of a Hoffman electrolysis apparatus with two stable atmospheric glow discharge as plasma electrode has been successfully in synthesis of silver and gold nanoparticles[27]. Conventional plasma spray has been applied to produce aluminia and zirconia nanomaterials[28], and atmospheric pressure plasma jet has been reported in synthesis of carbon nanomaterials[29].

2.3.3 Microwave in Nanoparticles synthesis

Microwaves are electromagnetic waves that move at the speed of light, and are reflected when they are used to irradiate a metal surface. By contrast, when they irradiate a dialectric material, various phenomena occur according to the nature of the electromagnetic waves. Figure 2.3 shows the summary of influence of electromagnetic waves on dialectric materials in various ranges of the electromagnetic spectrum.

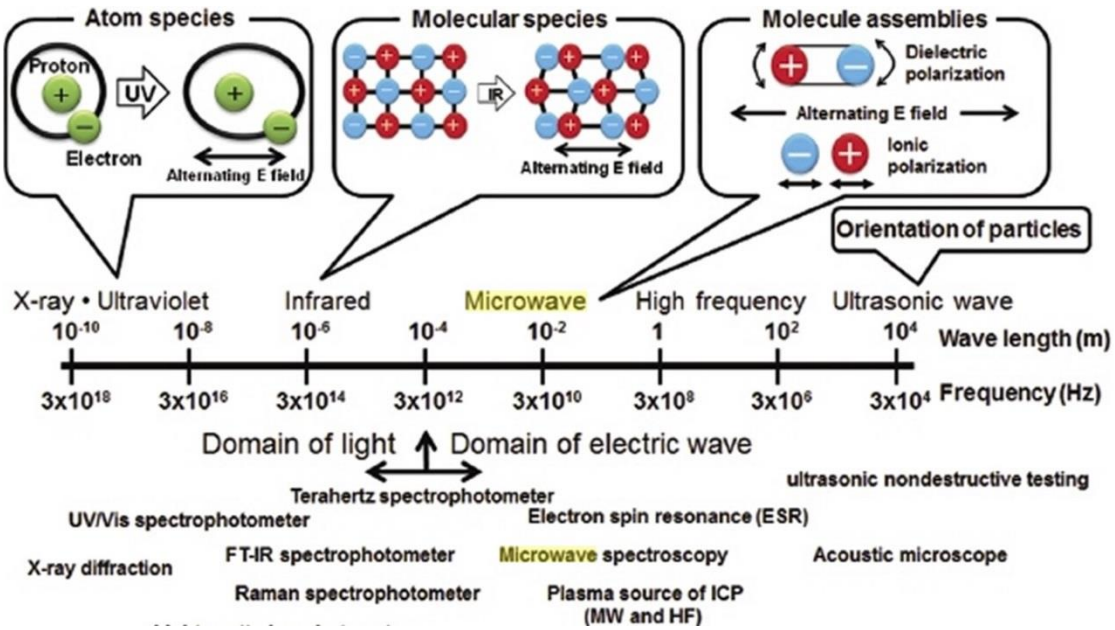

Figure 2.4 The resonance phenomenon of dielectric
(Source : Microwave in nanoparticle synthesis, John Wiley & Sons 2013)

In the domain of the microwave, the waveguide consisting of a metal tube, is used to transmit the microwaves. The cross-sectional size of the waveguide tube in figure 2.4 changes according to the frequency (wavelength) of the microwave radiation generated by the magnetron of the semiconductor generator. When metal plates (e.g short plunger) are attached to the extremities of the waveguide tube, the waveguide then transmits the microwave radiation at multiples of ½ waves tube.

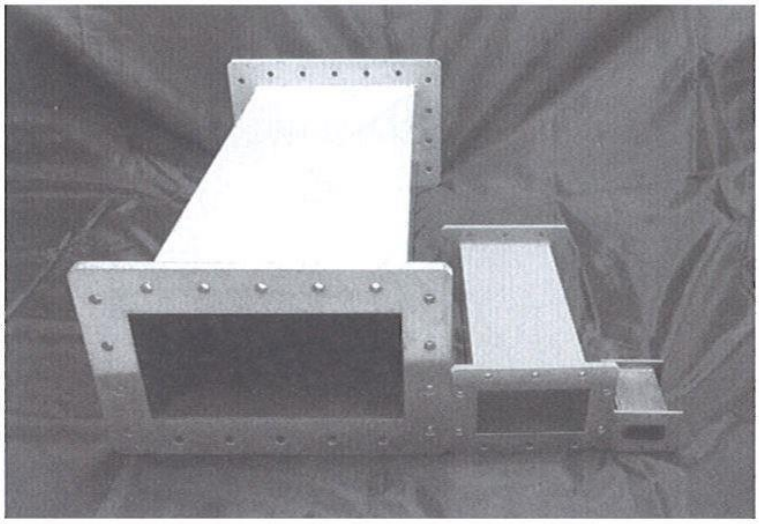

Figure 2.5 Waveguides used for 951-MHz microwaves (left), 2.45-GHz microwaves (center) and 5.8-GHz microwaves (right)
(Source : Microwave in nanoparticle synthesis, John Wiley & Sons 2013)

Much work in the field of microwave-assisted synthesis has been conducted using domestic microwave ovens. However, some problems exist in a domestic microwave system. For example, reactions are hard to control. It is particularly hazardous if flammable solvent and reagents are used. Moreover, it is very difficult to measure the temperature and microwave power accurately. With the advent of the scientific microwave system, these problems can be overcome. The commonly used microwave generator is 2.45 GHz of frequency. There are two mechanisms of interaction between materials and microwaves: dipole interaction and ionic conduction. Both mechanism require effective coupling between components of the target material and the rapidly oscillating electrical field of the microwaves. Figure 2. 5 shows a schematic illustration of the microwave interaction with polar H_2O molecules[4].

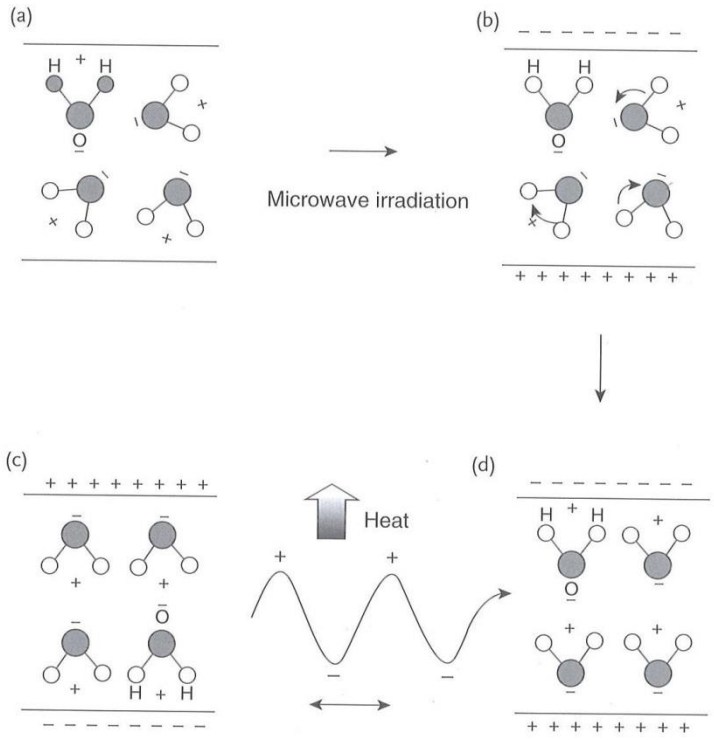

Figure 2.6 Schematic illustration of microwave interaction with polar H2O molecules (Source : Microwave in nanoparticle synthesis, John Wiley & Sons 2013)

Unlike conventional heating, microwave internal heating can prevent formation of a metallic on the synthesis reactor walls in nanoparticle synthesis, and plays an important role in the wash-free, continuous flow production of metallic nanoparticles. Microwave liquid plasma system can produce gold, silver, and platinum nanoparticles in mass production[4]. Hattori et.al reported synthesis of zinc and zinc oxide nanoparticles by microwave of 250 W with production rate at

3.3 g/h[15]. While using 2.45 GHz microwave plasma in liquid, continuous synthesis of magnesium-hydroxide, zinc oxide, and silver nanoparticles was obtained with higher productivity (production rate) and efficiency (production amount per energy) compared with pulsed laser ablation in liquid[16].

2.4. Conclusion

Nanoparticles are often defined as particles of less than 100 nm in diameter. Nanoparticles are of interest because of the new properties (such as chemical reactivity and optical behavior) that they exhibit compare with larger particles of the same materials. There are a wide variety of techniques that are capable of creating nanostructure with various degrees of quality, speed and cost.

Liquid phase method in synthesizing nanoparticles has many advantages rather than other method. Assisted with microwave generator, nanoparticles can be produces in mass production and high production rate.

Lastly, an overview of plasma-assisted technique based on the electrical discharge in liquid for synthesis of some metal nanoparticles have been described.

References

[1] Science Policy, "Nanoscience and nanotechnologies: opportunities and uncertainties," 2004.

[2] W. Luther, "Application of Nano- technologies in the Energy Sector," 2008.

[3] R. Luque and R. Varma S, Eds., *Sustainable Preparation of Metal Nanoparticles: Methods and Applications*, vol. 10. Royal Society of Chemistry, 2012, p. 230.

[4] S. Horikoshi and N. Serpone, Eds., *Microwaves in Nanoparticle Synthesis: Fundamentals and Applications*. John Wiley & Sons, 2013.

[5] F. J. Heiligtag and M. Niederberger, "The fascinating world of nanoparticle research," *Materials Today*, vol. 16, no. 7–8, pp. 262–271, Jul. 2013.

[6] M. Dragomir, "Metallic Nanoparticles," pp. 1–50, 2009.

[7] Y. Zhang, R. Huang, X. Zhu, L. Wang, and C. Wu, "Synthesis, properties, and optical applications of noble metal nanoparticle–biomolecule conjugates," *Chinese Science Bulletin*, vol. 57, no. 2–3, pp. 238–246, Jan. 2012.

[8] M. Oyama, A. Ali Umar, M. Mast Saleh, and B. Yeop Majlis, "Chemical Synthesis of Metal Nanoparticles in Aqueous Solutions with the Presence of Some Additives," *Sains Malaysiana*, vol. 40, no. 12, pp. 1345–1353, 2011.

[9] V. Sanchez-mendieta and A. R. Vilchis-nestor, *Green Synthesis of Noble Metal (Au , Ag , Pt) Nanoparticles , Assisted by Plant-Extracts*. InTech.

[10] N. Kulkarni and U. Muddapur, "Biosynthesis of Metal Nanoparticles: A Review," *Journal of Nanotechnology*, vol. 2014, pp. 1–8, 2014.

[11] V. V Makarov, a J. Love, O. V Sinitsyna, S. S. Makarova, I. V Yaminsky, M. E. Taliansky, and N. O. Kalinina, "'Green' nanotechnologies: synthesis of metal nanoparticles using plants.," *Acta naturae*, vol. 6, no. 1, pp. 35–44, Jan. 2014.

[12] N. V. Tarasenko, a. V. Butsen, and E. a. Nevar, "Laser-induced modification of metal nanoparticles formed by laser ablation technique in liquids," *Applied Surface Science*, vol. 247, no. 1–4, pp. 418–422, Jul. 2005.

[13] M. Tsuji, M. Hashimoto, Y. Nishizawa, M. Kubokawa, and T. Tsuji, "Microwave-assisted synthesis of metallic nanostructures in solution.," *Chemistry (Weinheim an der Bergstrasse, Germany)*, vol. 11, no. 2, pp. 440–52, Jan. 2005.

[14] W.-H. Chiang and R. M. Sankaran, "Microplasma synthesis of metal nanoparticles for gas-phase studies of catalyzed carbon nanotube growth," *Applied Physics Letters*, vol. 91, no. 12, p. 121503, 2007.

[15] Y. Hattori, S. Mukasa, H. Toyota, T. Inoue, and S. Nomura, "Synthesis of zinc and zinc oxide nanoparticles from zinc electrode using plasma in liquid," *Materials Letters*, vol. 65, no. 2, pp. 188–190, Jan. 2011.

[16] Y. Hattori, S. Mukasa, H. Toyota, T. Inoue, and S. Nomura, "Continuous synthesis of magnesium-hydroxide, zinc-oxide, and silver nanoparticles by microwave plasma in water," *Materials Chemistry and Physics*, vol. 131, no. 1–2, pp. 425–430, Dec. 2011.

[17] Y. Hattori, S. Nomura, S. Mukasa, H. Toyota, T. Inoue, and T. Usui, "Synthesis of tungsten oxide, silver, and gold nanoparticles by radio frequency plasma in water," *Journal of Alloys and Compounds*, vol. 578, pp. 148–152, Nov. 2013.

[18] Y. Hattori, S. Nomura, S. Mukasa, H. Toyota, T. Inoue, and T. Kasahara, "Synthesis of tungsten trioxide nanoparticles by microwave plasma in liquid and analysis of physical properties," *Journal of Alloys and Compounds*, vol. 560, pp. 105–110, May 2013.

[19] N. Toshima, "Metal nanoparticles for catalysis," 1950.

[20] F. Fi, G. Viau, and G. Shafeev, "Nanoparticles of metal and metal oxides : some peculiar synthesis methods , size and shape control , application to catalysts preparation," *Brazilian Journal of Physics*, vol. 39, pp. 134–140, 2008.

[21] G. Kawamura, M. Nogami, and A. Matsuda, "Shape-Controlled Metal Nanoparticles and Their Assemblies with Optical Functionanlities," *Journals of Nanomaterials*, p. 17, 2013.

[22] N. S. & M. K. H. Ghomia*, M. Yousefia, "Ultrasonic-assisted spark plasma discharge for gold nanoparticles synthesis," *Radiation Effects and Defects in Solids: Incorporating Plasma Science and Plasma Technology*, 2013.

[23] Y. Yang, Y. I. Cho, and A. Fridman, *Plasma Discharge in Liquid*. Taylor & Francis Group, 2012.

[24] G. Saito, "Solution Plasma Synthesis of Nanomaterial," Hokkaido University.

[25] R. M. Sankaran, Ed., *Plasma Processing of Nanomaterials*. CRC Press Taylor and Francis Group, 2011, p. 432.

[26] E. Omurzak, J. Jasnakunov, N. Mairykova, A. Abdykerimova, A. Maatkasymova, S. Sulaimankulova, M. Matsuda, M. Nishida, H. Ihara, and T. Mashimo, "Synthesis Method of Nanomaterials by Pulsed Plasma in Liquid," *Journal of Nanoscience and Nanotechnology*, vol. 7, no. 9, pp. 3157–3159, Sep. 2007.

[27] N. Shirai, S. Uchida, and F. Tochikubo, "Synthesis of metal nanoparticles by dual plasma electrolysis using atmospheric dc glow discharge in contact with liquid," *Japanese Journal of Applied Physics*, vol. 53, no. 046202, pp. 1–5, 2014.

[28] J. Karthikeyan, C. C. Berndt, J. Tikkanen, S. Reddy, and H. Herman, "Plasma spray synthesis of nanomaterial powders and deposits," *Material Science & Engineering A*, vol. 238, pp. 275–286, 1997.

[29] J. Kim, H. Sakakita, H. Ohsaki, and M. Katsurai, "Microwave-excited atmospheric pressure plasma jet with wide aperture for the synthesis of carbon nanomaterials," *Japanese Journal of Applied Physics*, vol. 54, no. 01AA02, pp. 1–5, 2015.

Chapter 3

Metallic zinc air battery

3.1 Introduction

At a time when a progressive transition from the internal-combustion engine vehicle to the electric vehicle was already commenced, they hope to reduce reliance on oil production and minimize CO_2 emissions are leading to a worldwide interest in high-energy density power sources. Current high-performance batteries barely provide sufficient energy to meet the challenges of next-generation technologies, forcing battery performance than is currently available. During the past two decade, lithium-ion technology as one of the most popular types of rechargeable battery, has almost reached its theoretical limit. The chase of next-generation rechargeable high-energy density batteries has led to great interest in metal-air battery technology[1].

Rather than lithium-ion batteries, metal-air batteries have the potential to save more energy, which are now used in electric vehicle and some grid application. Metal-air batteries could also be less expensive than lead-acid batteries, the cheapest, widely used rechargeable batteries based on material used. Table 3.1 summarizes the major advantages and disadvantages of the metal-air battery system[2]

Table 3.1 Major advantages and Disadvantages of Metal-Air Batteries

Advantages	Disadvantages
High energy density Flat discharge voltage Long shelf life (dry storage) No ecological problems Low cost (on metal use basis) Capacity independent of load and temperature when within operating range	Dependent on environmental conditions: Drying-out limits shelf life once opened to air Flooding limits power output Limited power output Limited operating temperature range H_2 from anode corrosion Carbonation of alkali electrolyte

As a result of their high theoretical energy densities, compared with other chemical-based batteries, metal air-batteries can contribute greatly to address the problems concerned in the fast growth of application, specificcaly in the fields of ekectric and hybrid-electric vehicle[3].

Due to the energy density is extremely high compared to that of other rechargeable batteries, metal-air batteries have attracted much attention as a possible alternative. A remarkable characteristic of metal-air batteries is their open-cell structure, since these batteries use oxygen gas gained from the air as their cathode material. Typically, metal-air batteries are divided into two kinds according to their electrolytes. One is a cell system using an aqueous electrolyte; such a system is not sensitive to moisture. The other is a water-sensitive system using an electrolyte with aproctic solvents. This system is degraded by moisture[4].

3.2 Metal Air Batteries

Metal-air batteries are related to the atmosphere, and need this access to operate. These characteristics make them distinctive from conventional batteries. Metal-air batteries are also different from fuel cell because metal-air batteries have a self-contained anode within the battery case itself. Metal-air batteries are part "conventional" battery and part fuel cell, sometimes they are called semi-fuel cells. "Conventional" batteries have the active component of both the anode and cathode within the battery case (see figure 3.1). The fuel cell has both "active" components (or fuels) of the anode and cathode supplied from outside the fuel

cell case. A metal–air battery, or semi–fuel cell, has the solid anode within the case (like a battery), while the cathode fuel is brought to the cell (like a fuel cell)[5].

Attractive metal–air systems are using metal electrodes with low equivalent mass and thus a theoretical specific charge. The data given in Table 3.1 show that this is especially the case for lithium and aluminium. Among these metals, zinc has the lower equivalent weight, the lowest ecological concern, and a very attractive cell voltage in conjunction with an oxygen electrode. The zinc–air battery system can be regarded as a sustainable and very promising power source[6].

Some metals can be used in metal/air batteries. Table 3.2 shows some electrochemical parameters, as well as those of a typical metal hybrid. Some typical figures for metal hybrid electrode are also provided in this table, which basically could be used as a negative electrode in battery with an air electrode as the positive electrode[7].

Table 3.2. Theoretical electrochemical parameters of electrode materials of interest for metal-air battery (Source : Liu.et.al, 2011,pp 203)

Electrode material	Equivalent mass[b] (g)	Specific. charge[b] ($Ah\,kg^{-1}$)	Standard electrode potential (V)	Electrode potential[c] at pH 14 (V)	Theoretical metal/O_2 cell voltage[c] (V)
Al	25.99	1032	−1.66	−2.38	2.78
Cd	73.20	366	−0.40	−0.80	1.20
Fe	44.92	597	−0.44	−0.87	1.27
Li	23.94	1120	−3.04	−3.04	3.44
MeH_x^a	70.00	370	0.00	−0.83	1.23
Mg	29.16	919	−2.38	−2.70	3.10
Na	39.98	671	−2.71	−2.71	3.11
Zn	40.69	659	−0.49(pH 0)	−1.26	1.67
O_2	8.00	3350	1.23	0.401	–

[a]Approximate values for the equivalent mass and theoretical specific energy in AB_5 alloys, such as $LaNi_5$.
[b]Equivalent mass is here calculated with respect to the product of discharge (e.g., $Al(OH)_3$, rather than Al ($MW_{Al(OH)3}$: 77.98 $g\,mol^{-1}$, EM: 77.98/3 = 25.99 g).
[c]Referring to the stable form of the discharge product reported in the Pourbaix diagram.

Metal-air batteries are open system. Just like in fuel cells, the air and water vapor can diffuse through the porous oxygen electrodes. Control of both the humidity and the carbon dioxide content of the air may be necessary for large-scale unit.

For metal-air batteries, many metals have been investigated as anode material and the main four are: aluminium, lithium, magnesium, and zinc. Magnesium and aluminium have low equivalent masses and hence a high theoretical value of the specific charge. They also have an anode instability, corrosion, or dissolution problems. Zinc has dissolution problems and a relatively low operating voltage. Lithium used in metal-air batteries with

aqueous electrolyte exhibits the problems of high self-discharge, parasite corrosion, and safety problems.

Zinc has received the most consideration of the potential metal-air battery candidates, because it is electropositive metal, which is relatively stable in aqueous and alkaline electrolytes without significant corrosion. It has been used over many years in commercial primary zinc-air batteries. A promising high-capacity power source for many portable applications as well as in larger sizes, for electric vehicles will achieve with the development of practical rechargeable zinc-air battery with an extended cycle life.

3.3. Nanotechnology for batteries

Recently, there has been much interest to the application of nanotechnology structure applied to new battery technology to improve metal-air battery efficiency. Material with proper nano-scale dimensions has the potential to dramatically enhance the transport of electrons, ions, and molecules associated with cycling of batteries, significantly accelerating the rate of chemical and energy transformation processes. The chemical reactivity of materials may critically be influenced by the large surface free energy, surface defects, and surface states.[8].

Cui et al. have observed the performance of lithium-ion battery using silicon nanowire and hollow nanoparticles. It was found that batteries containing these double walled silicon nanotube anodes exhibit charge capacity approximately eight times larger than conventional carbon anodes and charging rates of up to 20C (a rate of 1C corresponds to complete charge or discharge in one hour). [9]

By using nanostructured FeS_2 as the cathode material in the Li thermal batteries, the electrode materials react more rapidly and completely during discharge which produces the remarkable increase if energy output. Using nanostructured materials also made thermal batteries more compact and robust with higher energy density.[10]

Dai et.al reported an advanced zinc-air battery with higher catalytic activity and durability. A number of high-performance electrocatalysts made with non-precious metal oxide or nanocrystals hybridized with carbon nanotubes. These catalysts produced a higher catalytic activity and durability in alkaline electrolytes than catalysts made with platinum and other precious metals. A combination of a cobalt-oxide hybrid air catalyst for oxygen reduction

and a nickel-iron high-energy efficiency for a zinc-air battery, with a high specific energy density more than twice that of lithium-ion technology[11].

3.4 Zinc-air batteries

Zinc as a metal is a safe material and can be fully recycled. The availability of zinc has been increasing despite the growing zinc demand. The international Lead Zinc Study Group (ILZSG) reports 6 819 000 metric ton of zinc mined worldwide in 1994. According to the US. Geological Survey, the world's zinc reserves in 2005 were 220 000 000 metric ton and mining output reached 10 000 000 mt[6].

For practical applications, the most promising system available up to now and in the foreseeable future is the zinc-air system owing to its energy density, availability, price, and environmental compability of all components are strong argument for this battery[7].

Zinc has been used in batteries for decades as an active material for anode. It provides the highest specific energy among the various practical metal-air system.

Zinc-air batteries have long been recognized for their theoretical specific energies and low material costs. The inherent irreversibility of air electrodes

leads to low-to-moderate energy efficiencies for zinc-air batteries, with projected value of about 60%[12]

3.4.1 Working Principles of Zinc-Air Battery

Zinc air batteries are composed of three parts, zinc metal as an anode, an air electrolyte as the cathode, which is divided into a gas diffusion layer and a catalyst active layer, and a separator. Figure 3.1 shows working principle and each electrode reaction of zinc-air battery. The red circle in the picture shows three phase reaction (oxygen (gas), catalyst (solid), and electrolyte (liquid)) occurs in air cathode[4].

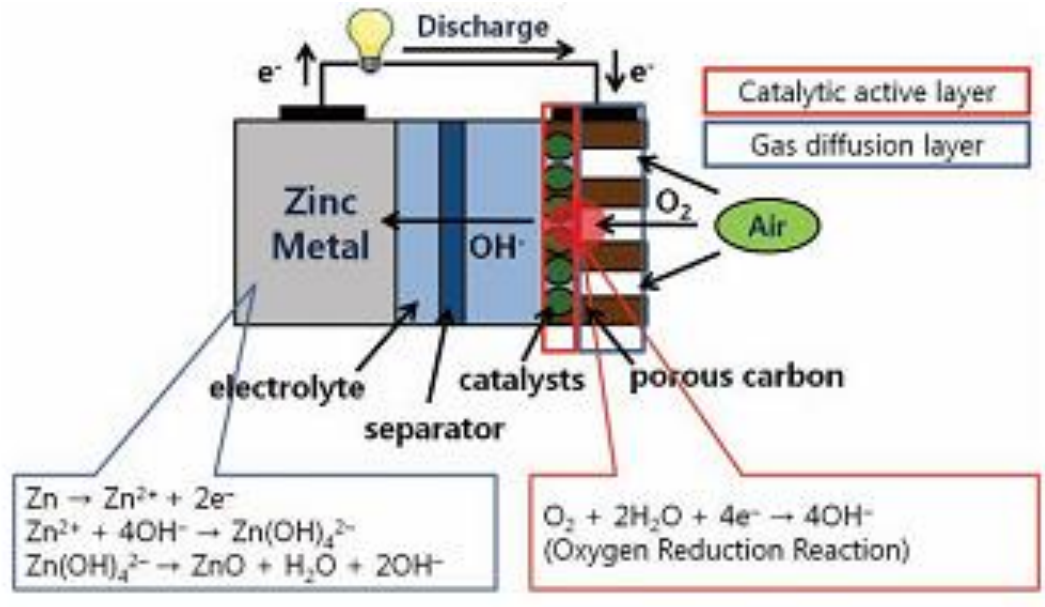

Figure 3.1. Working principle and each electrode reaction of zinc air battery (Source : Cho.et.al, 2011, pp35)

Zinc–air batteries use oxygen from the ambient atmosphere to produce electrochemical energy. Upon opening the battery to air, oxygen diffuses into the cell and is used as the cathode reactant. The air passes through the cathode active surface in contact with the cell's electrolyte.

Oxygen from the atmosphere diffuses into the porous carbon electrode by the difference in pressure of oxygen between the outside and inside of the cell, and then the catalyst facilitates the reduction of oxygen to hydroxyl ions in the alkaline electrolyte with electrons generated from the oxidation of zinc metal as the anode reaction. The overall procedure during discharge can be described as the following electrochemical reactions of anode and cathode in alkaline solution, respectively.

Anode : $Zn \rightarrow Zn^{2+}\ 2e^-$

: $Zn^2{}_+ + 4OH^- \rightarrow Zn(OH)_4{}^{2-}$

: $Zn(OH)_4{}^{2-} \rightarrow ZnO + H2O + 2OH–$

: $Zn + 2H_2O \rightarrow Zn(OH)_2 + H_2 \uparrow$

Cathode : $O_2 + 2H_2O + 4e^- \rightarrow 4OH^-$

Overall reaction : $2Zn + O_2 \rightarrow 2ZnO$

At the active surface, the air cathode catalytically promotes the reduction of oxygen in the presence of an aqueous alkaline electrolyte. The catalytic air electrode is not consumed or changed in the process. Since one active material lies outside of the cell, the majority of the cell's volume contains the other active component (zinc), thus on a unit volume basis, zinc-air batteries have a very high density[2].

3.4.2 Zinc-air battery for electric vehicle

The types and number of applications requiring improved or advanced rechargeable batteries are constantly expanding. In additions, the performance, life and cost requirements for the batteries used in many of these new and existing applications are becoming increasingly more rigorous. Commercially available batteries may not be able to meet these performance requirements. Thus, a need exists for both conventional battery technologies with improved performance and advanced battery technologies with characteristics such as high energy and power densities, long life, low cost, little or no maintenance, and a high degree of safety.

Battery performance for electric vehicle require specific properties, such as high specific energy and energy density to provide an adequate vehicle

driving range, high power density to provide acceleration, long life cycle with little maintenance and low cost. On the other hand battery for hybrid electric vehicles require a very high specific power and power density to provide acceleration, capable of accepting high power repetitive charges from regenerative braking, very long cycle life with no maintenance under shallow cycling conditions and moderate cost.

The U.S. Advanced Battery Consortium (USABC) established primary and secondary criteria for mid-term and long-term electric-vehicle batteries as seen in table 3.3. and 3.4.[2]. Three types of vehicles are selected here for use in discussing battery designs: a light duty electric van, a high-performance passenger car, and a hybrid vehicle. These three vehicle span the range of power to energy ratio being considered for on-road transportation vehicles that utilize battery energy storage.

Table 3.3. U. S. Advanced Battery Consortium Primary Criteria for Mid-Term and Long-Term Advanced Battery Technologies (Source : US Advance Battery Concortium)

Primary criteria	Mid term	Long term
Power density, W/L	250	600
Specific power, W/kg (80% DOD/30 s)	150 (200 desired)	400
Energy density, Wh/L (*C*/3 discharge rate)	135	300
Specific energy, Wh/kg (*C*/3 discharge rate)	80 (100 desired)	200
Life, years	5	10
Cycle life, cycles (80% DOD)	600	1000
Power and capacity degradation, % of rated spec.	20	20
Ultimate price, $/kWh (10,000 units at 40 kWh)	<150	<100
Operating environment, °C	−30 to 65	−40 to 85
Recharge time, h	<6	3–6
Continuous discharge in 1 h, % of rated energy capacity (no failure)	75	75

Table 3.4. U. S. Advanced Battery Consortium Secondary Criteria for Mid-Term and Long-Term Advanced Battery Technologies (Source : US Advance Battery Concortium)

Secondary criteria	Mid term	Long term
Efficiency, % (*C*/3 discharge, 6-h charge)	75	80
Self-discharge, %	<15 in 48 h	<15 per month
Maintenance	No maintenance; service by qualified personnel only	No maintenance; service by qualified personnel only
Thermal loss (for high-temperature batteries)	3.2 W/kWh 15% of capacity in 48-h period	3.2 W/kWh 15% of capacity in 48-h period
Abuse resistance	Tolerant; minimized by on-board controls	Tolerant; minimized by on-board controls

The zinc–air system can be mechanically recharged or may also be called refueling. The zinc–air battery can have additional zinc metal added to the battery as the anode material. Zinc may be added as a plate, powder, sphere, or

slurry. Mechanically recharging involves the pure metal anode or metal alloy designed for the system.

Besides the zinc–air battery as a mechanically rechargeable battery, it has been developed as electrically rechargeable battery either. Although both of them have been applied to electric vehicle applications, the trend is to use the mechanically rechargeable one. The electrically rechargeable zinc–air battery nominally operated at 1.2 V and delivers the specific energy of 180 Wh/kg, energy density of 160 Wh/I and specific power of 95 W/kg. The mechanically rechargeable zinc–air battery system represents a totally new design for electrically powered transportation having better performance characteristic, higher range and short charging time. In fact, it allows electric vehicle to perform nearly as well as internal combustion ones in terms of driving, speed, and acceleration, to refuel in only a few minutes and all those with no polluting emissions. In existing "fuel cell" batteries where the battery is recharged by physically replacing the zinc anodes, rather than by plugging it into a socket, the specific energy is 220 Wh/kg. Electrically rechargeable zinc–air batteries deliver 100 – 150 Wh/kg.

Electrically rechargeable zinc-air batteries rely on either a bifunctional air electrode, which must reduce O_2 on discharge and generate O_2 on charge, or a three-electrode system that includes an O_2 reduction electrode and O_2 evolution electrode. Zinc-air batteries have been configured to accept replacement of the Zn electrodes, that is , the battery is operated by adding metal particles in order to supply the active metal, and removing the ZnO reaction product as a highly-concentrated electrode phase or as a precipitated solid phase. This type of battery is called "mechanical rechargaeable"[12].

For mechanically rechargaeable batteries, 150 kWh batteries (800 kg) were fitted into several Mercedes-Benz transporter, giving them an autonomy of about 300 km with one battery charge. Electric Fuel Transportation Corporation made a cost forecast of 100\$kWh^{-1} of storage capacity, which would be far below the cost for conventional batteries. Most recently, Kummerow Corporation reported a record driving distance of 478 miles on single charge for their minivan equipped with a mechanically rechargeable zinc-air battery. While for electrically rechargeable zinc-air batteries, with their bifunctional air electrodes and pasted Zn electrodes a maximum cycle life of 450 cycles (3000 h) could be reached in 2.4 Ah test cells. Scale up of the battery components will lead to a 20

Ah/12V electrically rechargeable zinc–air battery offering a service life of ca. 2000 h (ca 2000 cycles)[7].

Another approach to powering electric vehicles with mechanically rechargeable zinc–air batteries is a hybrid configuration where the zinc–air battery is combined with a rechargeable battery such as a high–power lead–acid battery. With this approach the performance of each battery can be optimized.

3.5 Conclusion

Zinc is an environmentally friendly and easy–to–handle metal that is plentiful and can be readily recycled, therefore, the use of zinc as an electrode material in rechargeable and primary batteries would result in a sustainable battery technology.

An overview of the working principle of zinc air batteries was explained. Then application of nanotechnology to increasing battery efficiency is also described.

References

[1] J. Christensen, P. Albertus, R. S. Sanchez-Carrera, T. Lohmann, B. Kozinsky, R. Liedtke, J. Ahmed, and A. Kojic, "A Critical Review of Li/Air Batteries," *Journal of The Electrochemical Society*, vol. 159, no. 2, p. R1, 2012.

[2] D. Linden and T. B. Reddy, *HANDBOOK OF BATTERIES*, Third Edit. McGraw-Hill, 2001.

[3] M. Prabu, P. Ramakrishnan, H. Nara, T. Momma, T. Osaka, and S. Shanmugam, "Zinc – Air Battery : Understanding the Structure and Morphology Changes of Graphene-Supported CoMn 2 O 4 Bifunctional Catalysts Under Practical Rechargeable Conditions," *Applied Material & Interface*, no. 6, pp. 16545–16555, 2014.

[4] J.-S. Lee, S. Tai Kim, R. Cao, N.-S. Choi, M. Liu, K. T. Lee, and J. Cho, "Metal–Air Batteries with High Energy Density: Li–Air versus Zn–Air," *Advanced Energy Materials*, vol. 1, no. 1, pp. 34–50, Jan. 2011.

[5] S. L. Suib, Ed., *New and Future Developments in Catalysis: Batteries, Hydrogen Storage and Fuel Cells*. Newnes, 2013, p. 550.

[6] J. Van Wesemael and O. Haas, "Zinc – Air: Electrical Recharge," *Encyclopedia of Electrochemical Power Sources*. Elsevier, pp. 384–392, 2009.

[7] O. Haas, F. Holzer, K. M, and S. M, "Metal / air batteries : The zinc / air case," in *Handboook of Fuel Cells Fundamental Technology and Application*, John Wiley & Sons, 2010, pp. 1–27.

[8] M.-K. Song, S. Park, F. M. Alamgir, J. Cho, and M. Liu, "Nanostructured electrodes for lithium-ion and lithium-air batteries: the latest developments, challenges, and perspectives," *Materials Science and Engineering: R: Reports*, vol. 72, no. 11, pp. 203–252, Nov. 2011.

[9] H. Wu, G. Chan, J. W. Choi, I. Ryu, Y. Yao, M. T. McDowell, S. W. Lee, A. Jackson, Y. Yang, L. Hu, and Y. Cui, "Stable cycling of double-walled silicon nanotube battery anodes through solid-electrolyte interphase control.," *Nature nanotechnology*, vol. 7, no. 5, pp. 310–5, May 2012.

[10] Y. Chiang, "The Enabling Role of Nanomaterials in Lithium Battery Technology for Improved Energy Utilization."

[11] Y. Li, M. Gong, Y. Liang, J. Feng, J.-E. Kim, H. Wang, G. Hong, B. Zhang, and H. Dai, "Advanced zinc-air batteries based on high-performance hybrid electrocatalysts.," *Nature communications*, vol. 4, p. 1805, Jan. 2013.

[12] A. Landgrebe R and Z.-I. Takehara, Eds., "Proceedings of the Symposium on Batteries and Fuel Cells for Stationary and Electric Vehicle Applications," 1993, p. 341.

Chapter 4

Plasma in-Liquid Method for Reduction of Zinc Oxide in Zinc Nanoparticle Synthesis

4.1 Introduction

Metal-air batteries have attracted excitement recently due to their wide application in electric vehicles, next-generation electronics, as well for energy storage. Lithium, aluminum, iron, and zinc show great promise for use in air batteries. Among these kinds of metals, zinc, particularly as nanoparticles, has attracted great interest due to its low equivalent weight, abundance, and high-energy density [1]. Moreover, it is also safe and environmentally friendly [2-5]. However, in the zinc air battery, a combination of high-energy density of metal

anodes with atmospheric oxygen can lead to the formation of zinc oxide in large quantities [6–8].

Several morphologies of zinc, such as zinc nanoparticle [9,10], zinc nanowire [11,12], zinc nanofibers [13], zinc nanotube [14] and zinc nanosheets [12] were synthesized by various methods, including in-liquid plasma from zinc wire, laser ablation from zinc metal, electromagnetic levitation gas condensation from zinc, shortcut hydrothermal strategy synthesis from zinc acetate, Electron Cyclotron Resonance (ECR) plasma from zinc metal, ball-milling process from ZnO and amorphous boron, mechanical deformation process using hexagonal Zn oxide powder, simple thermal vapor phase deposition from zinc powder, metalorganic chemical vapor deposition from $Zn(C_2H_5)_2$ and thermochemical reduction from Zinc Sulfide (ZnS) powder.

Zinc oxide nanomaterial synthesis by zinc oxidation has been reported in numerous studies [15–21], but little research has been conducted into its reduction. It is necessary to balance zinc production with zinc recycling. The recycling of zinc is a critical and beneficial supplement to its primary metal production.

Additionally, zinc plays an essential role in preventing from decreasing energy use, minimizing emissions as well as reducing waste materials [22].

When microwave or radio-frequency-induced plasma is generated at the surface of a metallic electrode submerged into a liquid, nanoparticles are synthesized by erosion of the electrode. In-liquid plasma has been successful in the synthesis of many kinds of nanoparticles such as zinc, zinc oxide, tungsten oxide, silver, gold, and magnesium hydroxide to name a few [23,24]. By applying plasma to a zinc electrode in ethanol, metallic zinc nanoparticles are produced, while, in water, a mixture of zinc and zinc oxide nanoparticles is formed. This suggests that the oxidative or reductive atmosphere of the vapor of the liquid determined the physical properties of the synthesized nanoparticles. Plasma can be observed easily in the vapor, which was generated by the evaporation of the surrounding liquid.

The objective of this research is to reduce ZnO powder by microwave-induced plasma in ethanol, with the ethanol being the reducing agent. The synthesized materials were identified using an absorption spectrophotometer, energy-dispersive X-ray spectrometry (EDS) and X-ray diffraction (XRD) (M21X,

Mac Science), and as well as observed using a transmission electron microscope (TEM) (JEM-2100, JEOL).

4.2 Experimental Method

The apparatus used in this experiment is shown in figure 4. 1. The reaction vessel is a transparent polycarbonate tube with an inner diameter of 55 mm and outer diameter of 60 mm. A coaxial electrode consisting of an inner conductor of a sharpened copper rod 5 mm in diameter, dielectric Teflon, and outer conductor of brass, was placed perpendicular to the bottom of the vessel. The bottom of the vessel was tapered at an angle of 60 degrees to feed the ZnO powder efficiently to the top of the electrode where the plasma was generated. A copper tube 3 mm in outer diameter and 2 mm in inner diameter used as a counter electrode was placed 2 mm away from the coaxial electrode.

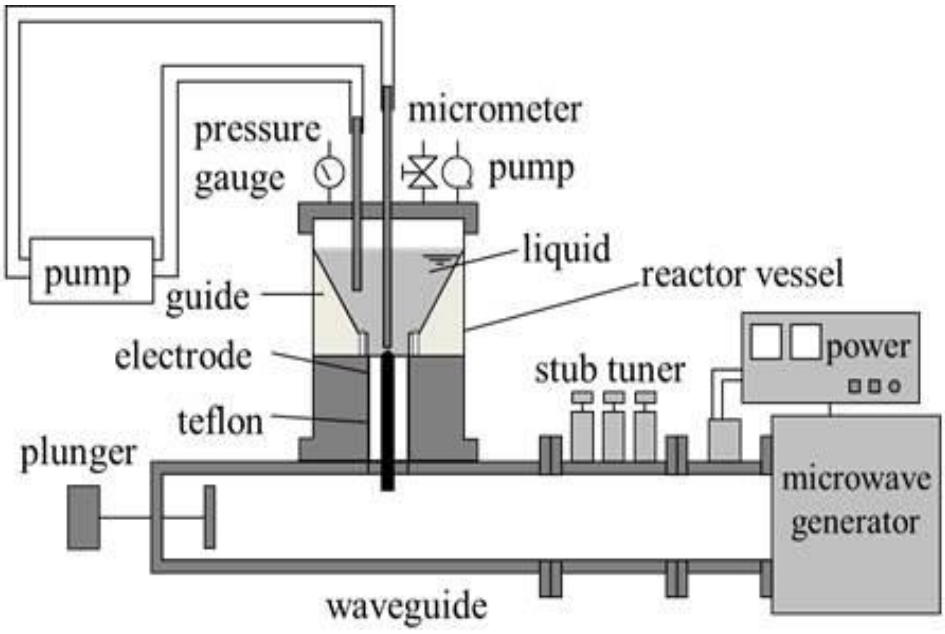

Figure 4.1 Experimental Apparatus

ZnO powder, labeled 200 mesh, 99.999% (NEWMET KOCH) was used. Two different concentrations were applied. For high density dispersion, 3.0 g, 5.0 g, and 6.0 g of ZnO powder were dissolved in 80 ml ethanol respectively. For low density dispersion, 0.1 g, 0.2 g, and 0.3 g of ZnO powder were used. It was initially stirred manually and then applied to an ultrasonic device until the powder was dispersed sufficiently. The dispersion was poured into the vessel and the pressure in the vessel was decreased to 30 kPa using an aspirator.

The liquid was circulated using a gear pump, and funneled from the counter electrode toward the top of the inner electrode.

A 2.45 GHz microwave in TE10 mode passed through a rectangular waveguide, was converted with in TEM mode and then subsequently passed through the coaxial electrode. By adjusting a plunger and stab tuner, the input power was increased until plasma ignition occurs between the coaxial electrode and counter electrode. After plasma ignition, the plasma was maintained at 235 W. The period of the plasma generation lasted ten minutes for low density dispersion, and eight and a half minutes for high density liquid dispersion. A different time of plasma generation was caused by liquid densities. When using a high density dispersion, the ZnO powder after a few minutes of plasma irradiation covers the tip of the electrode and making continuous plasma generation difficult to occur. With low density dispersion, the plasma remains stable until irradiation continued for 10 minutes, because there is no ZnO powder covers the tip of the electrode.

4.3 Result and Discussion

During plasma generation, the purple color of plasma emission was observed by naked eye, and the emission spectrum was measured using a spectroscope (PMA-11, HAMAMATSU). Characteristic Zn lines were detected at 468.0, 472.2 , 481.1 and 636.2 nm, and the excitation temperature was approximately 3400 K as estimated from emission intensity of these lines by the Boltzmann plot method. Among the three different amounts of ZnO powder (0.1 g, 0.2 g, and 0.3 g), the dispersion of 0.2 g was chosen to be the representative result for low density because at this dispersion, plasma was very stable and continuously presented a purple color which is recognized as the color of Zinc.

Figure 4. 2(a) shows the absorption spectroscopy of the 0.2 g dispersion as a function of time, from 0 minutes (before plasma generation) to 2, 4, 6, 8, and 10 minutes (after plasma generation) as taken by a spectrophotometer (UV-1800, Shimadzu). During plasma generation, there is a great reduction as the absorbance decreases. It can be seen near 360 nm and 380 nm wavelengths. The wide gap of ZnO between 320 and 390 nm has been reported for other techniques [25-28]. The

other peak observed around 200 to 250 nm on the short-wavelength side is believed to be the result of the formation of Zinc nanoparticles. Syntheses of Zinc nanoparticle from a zinc rod by plasma in a liquid were shown the same peak around 220 nm [24]. Research into nanoparticle synthesis by laser ablation has reported that a sharp peak for Zn nanoparticles appears at 232.4 nm [29] and simmilarly, it has reported around 230 nm for synthesis by radiation chemical reduction [30]. Since a peak in carbon has also been reported to appear around 230 nm, one of the peaks might be derived from Zn and another from carbon, however, this has not been clarified yet.

Figure 4. 2(b) shows peak height of the absorbance, which was obtained by subtracting the base of the peak from the peak value. On the short-wavelength side where a Zn peak is assumed to have been obtained, the peak height increased during the elapsed time of plasma generation. While on the long-wavelength side where a ZnO peak was observed, the peak height decreased. The Beer-Lambert law predicts that the intensity of an absorption peak is directly proportional to the concentration of the compound.

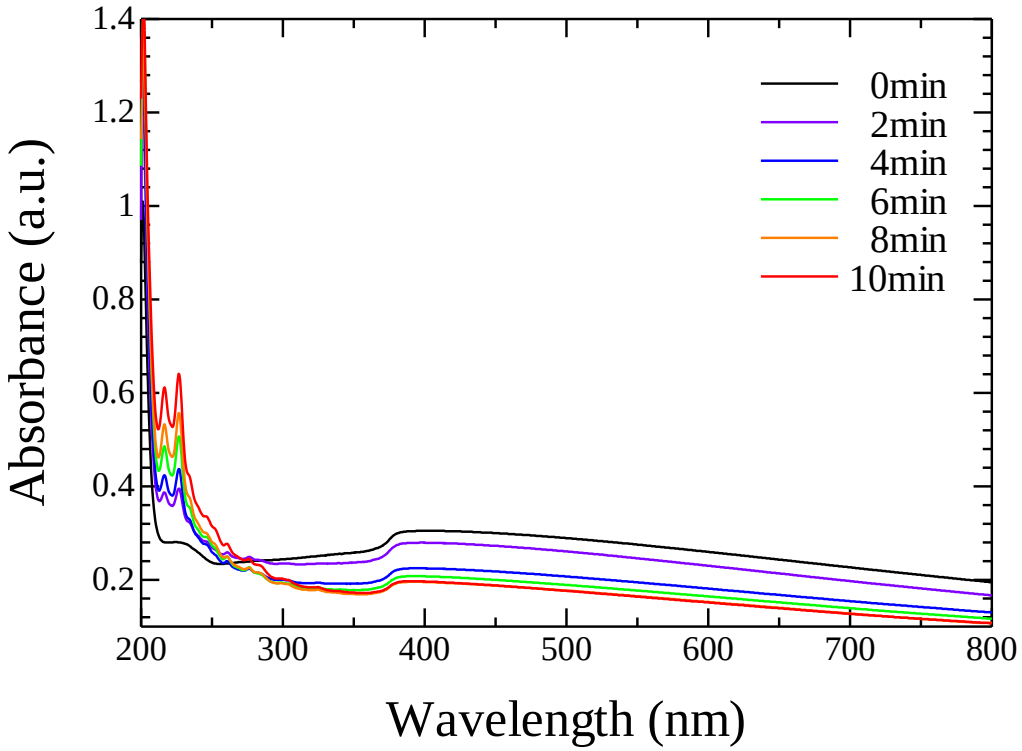

Figure 4. 2(a). Absorption spectroscopy

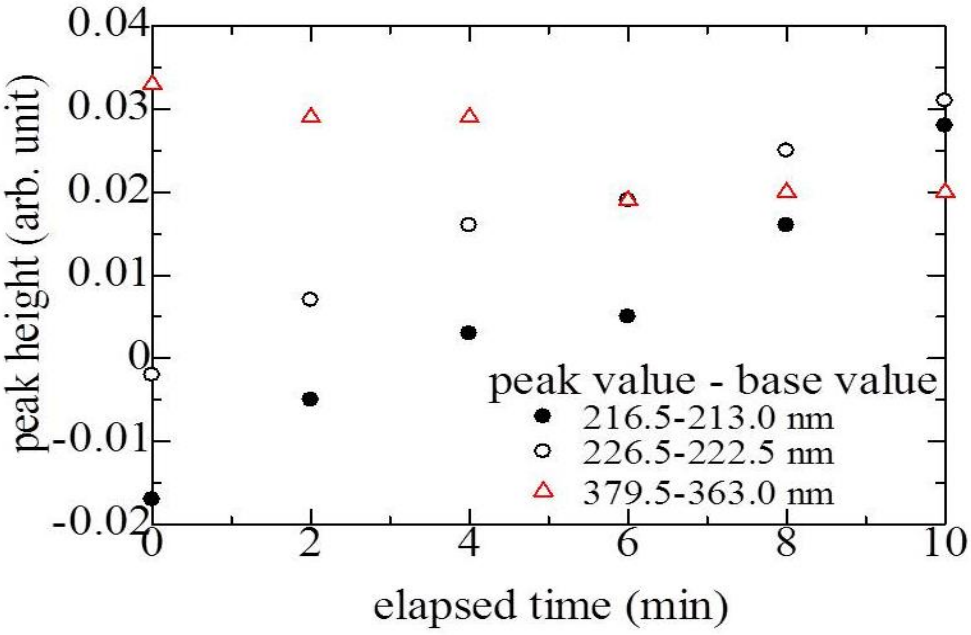

Figure 4. 2(b). The peak height for elapsed time of plasma generation

After plasma generation in the dispersion of 0.2 g ZnO in 80 ml of ethanol, the product adhered to the tip of the coaxial electrode is shown in figure 4. 3(a) and residue after evaporation of liquid is shown in figure 4. 3(b). The TEM images of the particles are shown in figure 4. ZnO nanoparticles before plasma generation were a mixture of rectangular and hexagonal crystals of 50 to 200 nm in length and rods approximately 200 nm in length as shown in figure 4. 4(a). TEM images of particles collected from the tip of the electrode, and from the residue after evaporation of liquid are shown in figures 4. 4(b) and (c) respectively. Good crystallinity of cubic particle about 30 nm- 200 nm in diameter is found from the tip of the electrode. It has been reported than zinc nanoparticles in cubic shape have been synthesized by plasma in liquid method using zinc wire [24]. Another rectangular particle is observed in the residue of liquid after evaporation. Although the particles seemed to be in crystalline form and similar to ZnO particles before plasma generation, the amount of oxygen after plasma generation was negligible according to the EDS spectrum in figures 4. 5(a) and (b). This EDS spectrum was conducted for nanoparticle collected at the tip of electrode, which is TEM image show different

shape from the ZnO TEM image before plasma irradiation. The mass ratio of oxygen to zinc was found to be 6% which were smaller than the theoretical value of ZnO which was approximately 24%.

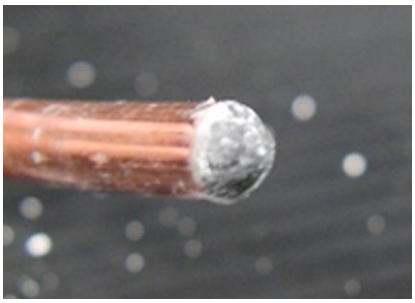

(a)

(b)

Figure. 4. 3(a). Product adhering to the tip of the electrode, 3(b) Residue after liquid evaporation

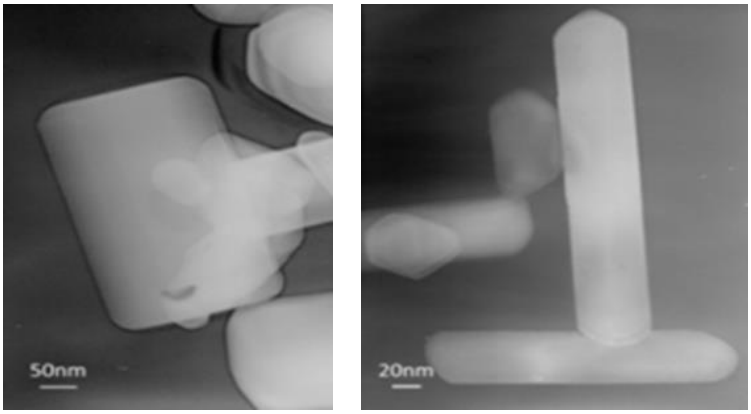

(a)

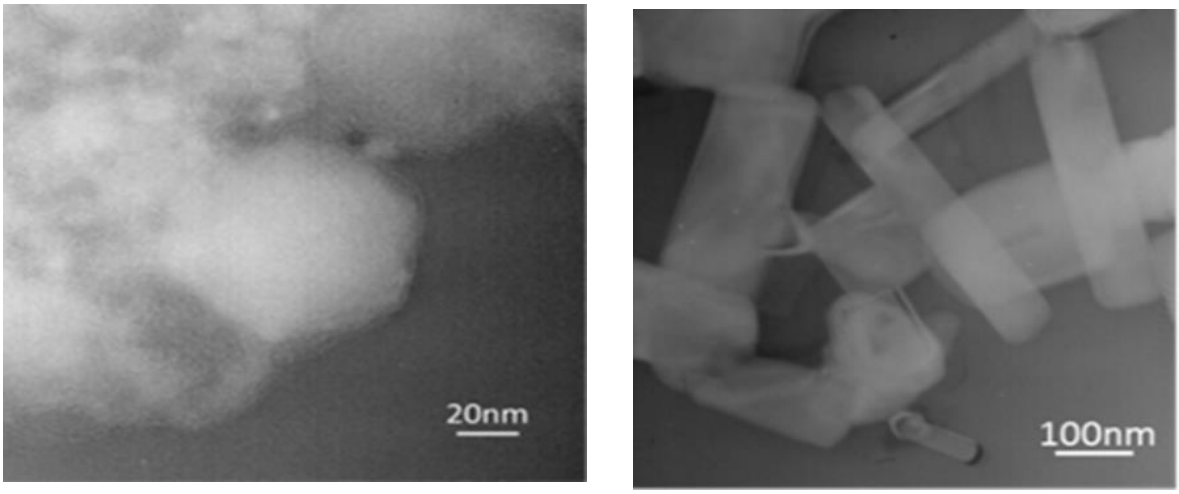

(b) (c)

Figure 4. 4. (a) TEM image of ZnO before plasma irradiation.
(b) TEM images of nanoparticles in the dispersion of 0.2 gm in 80 ml ethanol, Particles collected from the tip of the electrode.
(c) TEM image of particles from residue after liquid evaporation.

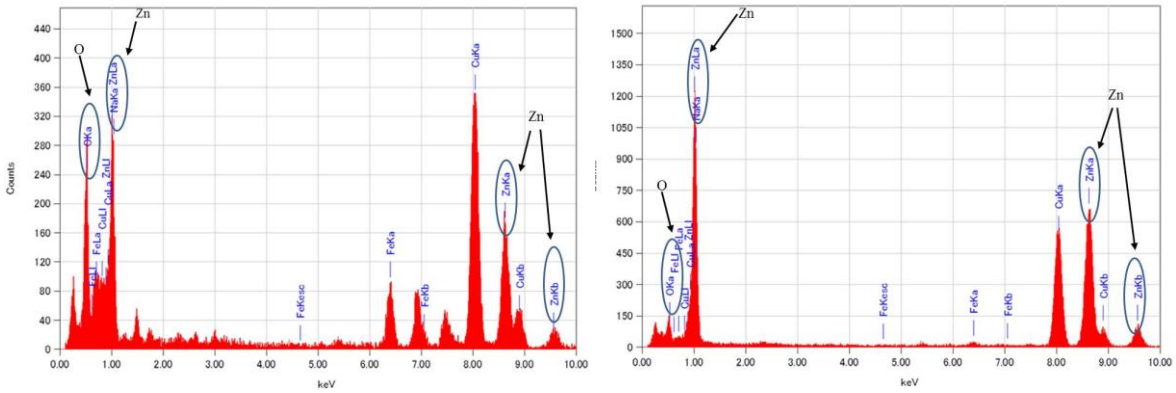

(a) (b)

Figure 4. 5. (a) EDS spectra in the dispersion of 0.2 gm ZnO before plasma irradiation. (b) After plasma irradiation.

There were no significant differences of particle synthesized when using 0,1 and 0.3 g of ZnO powder.

For high density dispersion, plasma generation at a dispersion of 6.0 g ZnO in 80 ml ethanol was relatively more stable than the dispersions of 3.0 g and 5.0 g of ZnO powder, even though the nanoparticles synthesized showed no significant difference in shape or size.

After plasma generation, TEM images of particle were found to show two types of particles, white polygonal ones and spherical fiber-flocculated ones as

shown in figure 4. 6(a). The diameter of the spherical particles was approximately 180 nm. From the enlarged image of the fiber-flocculated spherical particles in figure 4. 6(b), the diameter of one fiber was found to be approximately 10 nm. Figure 4. 7(a) shows the EDS spectrum of the white polygonal particles, sufficient oxygen was detected to determine that the particles consisted of ZnO. On the other hand, according to the EDS spectrum of the fiber-flocculate particles in figure 4. 7 (b), hardly any oxygen was present.

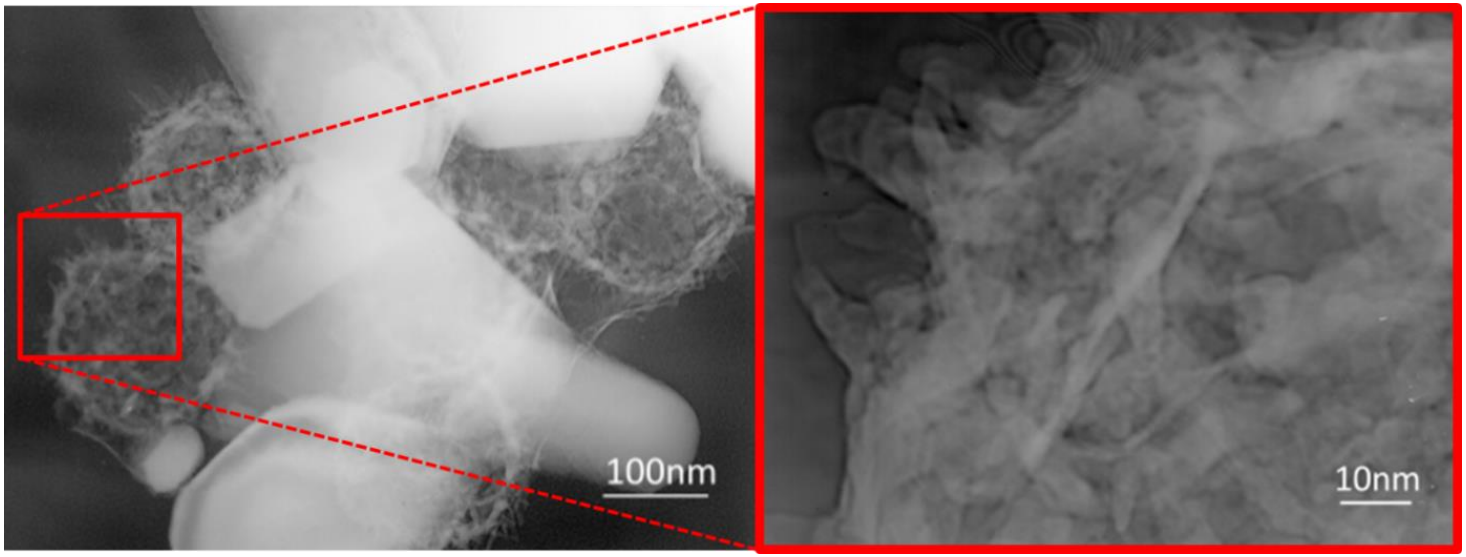

(a) (b)

Figure 4. 6. (a) TEM image of nanoparticle in the dispersion of 6.0 gm ZnO in 80 ml ethanol, (b) an enlarged image of a fiber-flocculate spherical particle

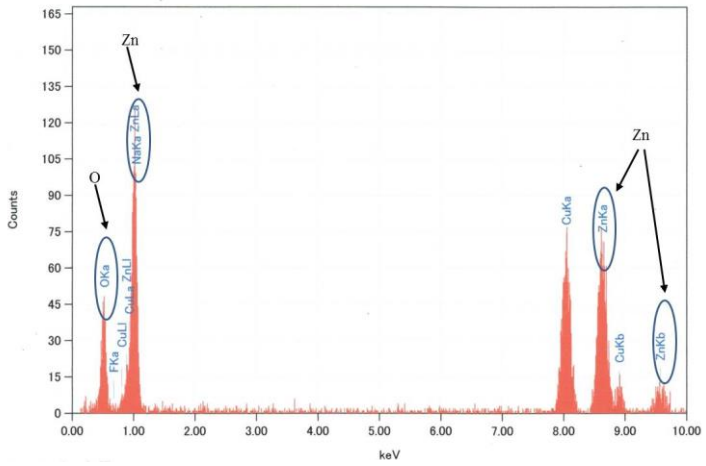

(a)

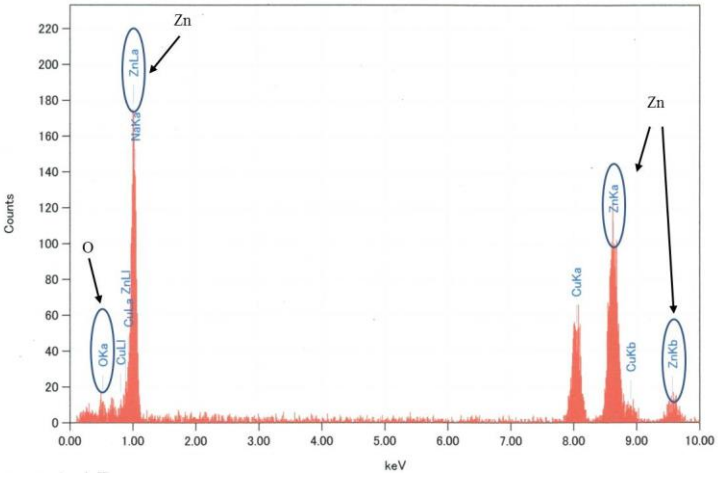

(b)

Figure 4. 7. (a) EDS spectra in the dispersion of 6.0 gm Zn in 80 ml ethanol before plasma irradiation. (b) after plasma irradiation.

Further investigations of the product were performed using x-ray diffraction (XRD). The XRD pattern before and after plasma generations for dispersion of 0.2 g and 6.0 ZnO powder are shown in figures 4. 8(a), (b), and (c) respectively. These spectra were recorded for a whole particle includes the

particle that remains in a liquid. Some metallic zinc peaks were observed after plasma generation, although ZnO was dominant.

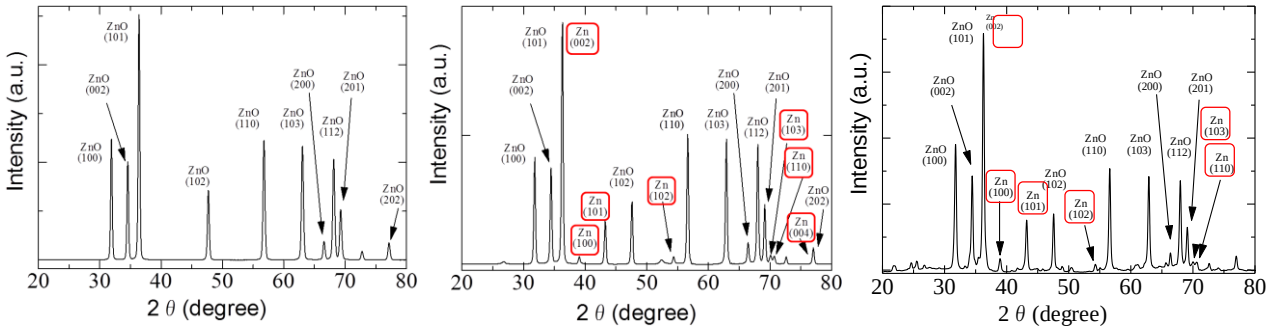

(a) (b) (c)

Figure 4. 8. (a) XRD pattern before plasma generation. (b) after plasma irradiation (6.0 g of ZnO), (c) after plama irradiation (0.2 g of ZnO)

Under the assumption of reduction due to thermal reaction, the reduction of ZnO is predicted using a consideration of chemical equilibrium and the Ellingham diagram.

The chemical equilibrium can be calculated from chemical potential of all the products. 27 species were given in the calculation as products from ethanol, O, H, H_2, O_2, H_2O, OH, HO_2, H_2O_2, C(g), C_2, C_3, CO, CO_2, C_3O_2, CH, CH_2, CH_3, CH_4, C_2H, C_2H_2, C_2H_4, CH_2O, CH_3OH, HCOOH, CH_2CO, CH_3HCO and C(s). The chemical potential of product p is expressed as follows:

$$\mu_p = \mu_p^0 + RT \ln P_p , \qquad (1)$$

Where $\mu_p{}^0{}_p$, R, T, and P_p are the chemical potential of p at standard condition, the gas constant, temperature, and the partial pressure of p, respectively. The $\mu_p{}^0$ of all the products can be calculated from JANAF thermochemical tables. When all the products are under chemical equilibrium, the chemical potential can be calculated from the three representative chemical potentials such as $\mu_{C(s)}$, μ_H, and μ_O as follows:

$$\mu_p = n_p^C \mu_{C(s)} + n_p^H \mu_H + n_p^O \mu_O \qquad (2)$$

Where $n^C{}_p$, $n^H{}_p$ and $n^O{}_p$ are the numbers of C, H and O atoms in p, respectively. 24 equations expressed as eq. 2 are made up for 24 products except for C(s), H and O. Because there are 27 indeterminate variables, which are chemical potentials, three more equations will be needed to solve them. The atomic ratios of C to H and of O to H have to be retained between the reactants and products expressed as,

$$\sum_p n_p^C \Big/ \sum_p n_p^H = \text{const.} \qquad (3)$$

$$\sum_p n_p^O \Big/ \sum_p n_p^H = \text{const.} \qquad (4)$$

The total pressure is a determinate value such as 30 kPa, expressed as,

$$\sum_p P_p = \text{const.} \tag{5}$$

If ethanol is used as a solvent, the values of the right side of eq. 3 and 4 become 1/3 and 1/6, respectively. Thus, 27 chemical potentials or partial pressures which follow the chemical potentials as expressed in eq. 1 can be calculated from eq 2–5.

An Ellingham diagram is used to predict whether the reaction of metals progresses to oxidation or reduction. If a metal oxide of metal M is expressed as M_xO_y, the reaction equation is expressed as follows:

$$\frac{2x}{y}\mathrm{M} + \mathrm{O}_2 \leftrightarrow \frac{2}{y}\mathrm{M}_x\mathrm{O}_y \tag{6}$$

The Ellingham diagram shows the Gibbs energy change ΔG^0 by 1 mole O_2 under the partial pressure of O_2 of 1 atm as a function of temperature. The Gibbs energy change ΔG of the reaction changes with the partial pressure of O_2 and is expressed as,

$$\Delta G = \Delta G^0 - RT \ln P_{O2} \tag{7}$$

The reaction shown in eq. 6 progresses from left to right when ΔG is negative, while inversely it progresses from right to left when ΔG is positive. A reducing atmosphere, that is, will be provided when ΔG is positive.

Some mole fractions of dominant products under the chemical equilibrium are shown in Figure 4. 9. The maximum mole fraction of O_2 is under 10^{-9}, and is much smaller than the dominant products. The Gibbs energy change of zinc oxidation is shown in figure 4. 10. ΔG increases with the temperature and turns to a positive from a negative at 1140 K. This indicates that if the temperature is higher than 1140 K, the reducing atmosphere is available for zinc oxide.

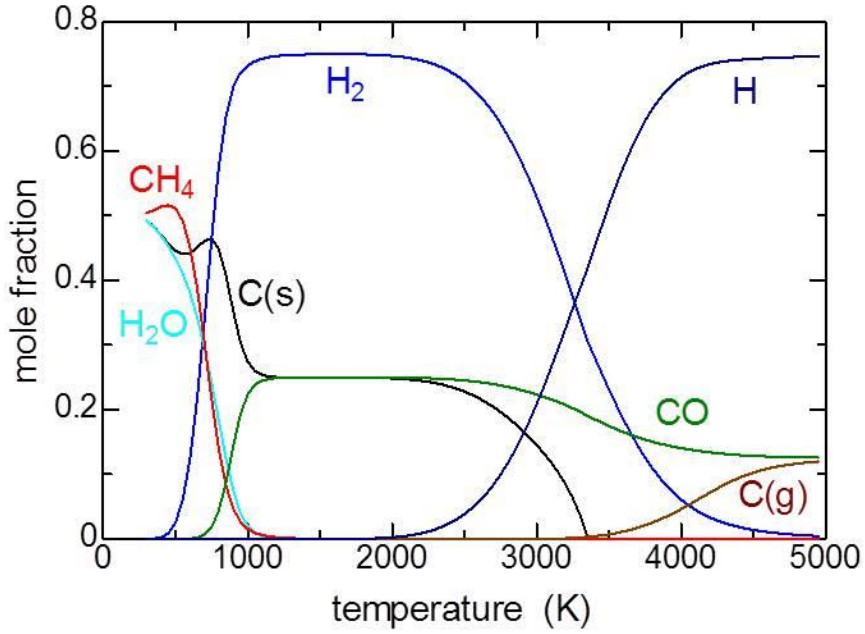

Fig.4. 9. Mole fraction of product

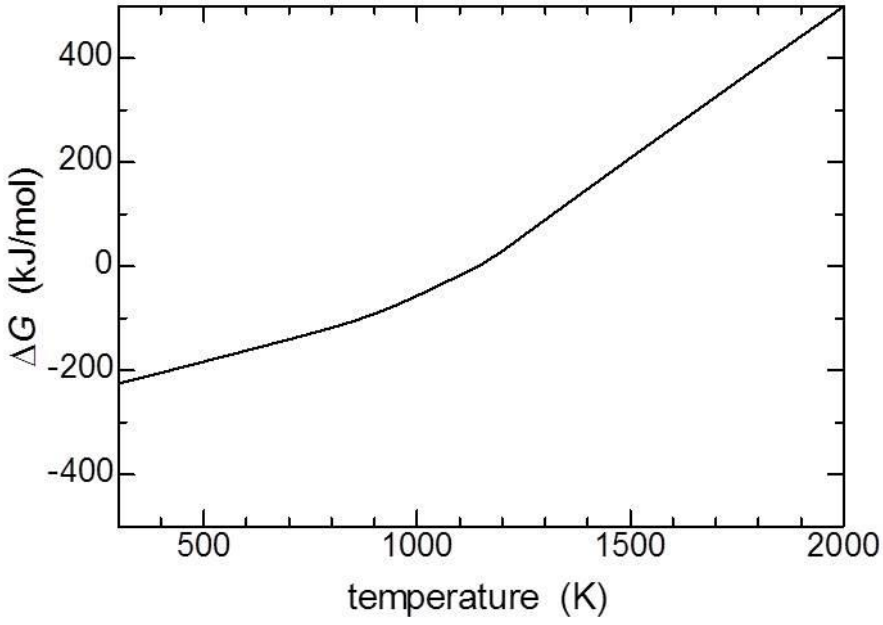

Figure. 4. 10. The Gibbs energy change of Zinc oxidation

In-liquid plasma may be suitable for generating a temperature of over 1140 K. It is difficult to measure the temperature, but spectroscopic measurement of plasma emission provides some important information concerning temperature. Line emission spectra of some species can give the excitation temperature through application of the Boltzmann plot method. The excitation temperature is related with the electron temperature. However, the electron temperature is not necessarily the same as the gas temperature, because in-liquid plasma is not necessarily in thermal equilibrium. The excitation temperature of in-liquid plasma is found to be generally between 3000 and 5000 K [31], and decreases with an increase of pressure. When plasma is generated in water, OH spectral band is detected around 310 nm. The rotational temperature of OH radicals can be obtained by matching the configuration of the spectral band to that of computational simulation. The rotational temperature is considered to be close to the gas temperature, because the thermal energy is almost equally distributed to the translation, rotational and vibrational energy of the molecule. The rotational temperature of in-liquid plasma was found to be generally from 3000 to 5000 K, [31, 32] and increases with the increase of pressure. Finally, the continuous spectrum of the black-body

radiation from the electrode can sometimes be detected. By fitting it to the Planck's law, the temperature of the electrode which is in contact with the plasma can be obtained. The temperature of the electrode was found to be roughly between 1300 and 1700 K [32, 33].

All the temperatures shown above exceed 1140 K. Therefore, the reaction field provided by the in-liquid plasma is a reducing atmosphere for zinc oxide.

When the 0.2 gm dispersion of ZnO was used, nearly all the ZnO particles in the dispersion were found to have been converted to Zn particles by the plasma. From this, the energy efficiency can be estimated, knowing that a reduction of 0.2 g (2.5 mmol) ZnO was caused by supplying microwave of 78 kJ to the plasma. From the theoretical enthalpy for reduction of ZnO of 348.3 kJ/mol, the energy efficiency of the present experiment becomes 1.1%, obtained by the following calculation.

$$\frac{348.3\,\mathrm{kJ/mol}\cdot 2.5\times 10^{-3}\ \mathrm{mol}}{235\,\mathrm{W}\cdot 330\,\mathrm{s}\,(=78\,\mathrm{kJ})}\times 100 = 1.1\% \qquad (8)$$

Pyrometallurgy and electrowinning are industrial processes comparable with the present experiment. Both processes require roughly 3000 kWh to 1 ton

of metallic zinc, and from these values, the energy efficiency of these processes can be calculated to be 49%.

Another method for Zinc recovery that has been reported, the hydrometallurgical method, uses methane and solar thermal technology [34-36] however, these methods has no information regarding the Zinc nanoparticle production that is needed for Zinc air batteries. This present method provides for recycling of Zinc nanoparticles with prevention of re-oxidation, because the reaction area is separated from the air by liquid. An additional advantage to this method is the easy collection of the product since the reduced metal remains in the liquid as dispersed particles.

From the calculation results, two parameters were derived theoretically for the proposed reduction method. One is that the appropriate ratio of ethanol and zinc oxide should be prepared for the plasma, and the other is that the temperature within the plasma should be between 1500 and 2000 K in order to utilize the enthalpy change of ethanol efficiency.

4.4 Conclusion

Zinc nanoparticles were synthesized from reduction of ZnO powder by 2.45 GHz microwave in ethanol, which act as reducing agents. Nanoparticles in cubic and hexagonal shapes of about 30 nm to 200 nm along with fiber flocculates 10 nm in diameter were found at the tip of the electrode and in the remaining liquid after plasma generation. This study was conducted simply to confirm the reduction of ZnO by plasma in liquids, and was not intended as an improvement of energy efficiency. In the future, in order to improve the energy efficiency, many parameters must be examined, for example, the type of liquid, frequency, power, pressure, arrangement of the device, and so on. Moreover, the distinctive nanoparticles synthesized by this experiment, and the mechanism of synthesis should be clarified in the future to get perfectly reduction of oxide and synthesize pure metallic Zinc nanoparticles.

References

[1] S. Peng, W. Du, L. Rakesh, A. Mellinger, and T. Kaya, Mater. Research Soc. **1440**, (2012).

[2] M. Bergman, Master Thesis, Division of Condensed Matter Physics, Chalmes University of Technology (2013).

[3] Y.-H. Wen, J. Cheng, S.-Q. Ning, and Y.-S. Yang, J. of Power Sourc. **188**, 301 (2009).

[4] J.-S. Lee, S. Tai Kim, R. Cao, N.-S. Choi, M. Liu, K.T. Lee, and J. Cho, Adv. Energy Mater **1**, 34 (2011).

[5] E. Moon, J. Kim, S. Nam, and S. Eom, Japanese J. Appl. Phys. **02**, 51 (2012).

[6] S.-H. Lee, Y.-J. Jeong, S.-H. Lim, E.-A. Lee, C.-W. Yi, and K. Kim, J. Korean Electrochem. Soc. **13**, 45 (2010).

[7] Y. Xu, X. Xu, G. Li, Z. Zhang, G. Hu, and Y. Zheng, Electrochem. Sci. **8**, 11805 (2013).

[8] A. Kraytsberg and Y. Ein-Eli, Nano Energy **2**, 468 (2013).

[9] Y. Hattori, S. Mukasa, H. Toyota, T. Inoue, and S. Nomura, Mater. Lett. **65**, 188 (2011).

[10] M. Vaghayenegar, a. Kermanpur, M.H. Abbasi, and H. Ghasemi Yazdabadi, Adv. Powder Tech. **21**, 556 (2010).

[11] V.S. Purohit, S.Ded, S. Kr. Bhattacharya, A. Kshirsagar, C.V. Dharmadhikari, S. V.Bhoraskar. Nucl. Instrum. Methods Phys. Res. Sect. B 266 (2008)

[12] Y.-C. Zhu and Y. Bando, Chem. Phys. Lett. **372**, 640 (2003).

[13] J. Hu, Z. Chen, J. Xie, and Y. Yu, J. Appl. Phys D, **41**, 032004 (2008).

[14] J. Li and X. Chen, Solid State Commun. **131**, 769 (2004).

[15] A.N. Hattori, M. Ichimiya, M. Ashida, and H. Tanaka, Appl. Phys. Express **5**, 125203 (2012).

[16] H. Fujisawa, R. Kuri, M. Shimizu, Y. Kotaka, and K. Honda, Appl. Phys. Express **2**, 055003 (2009).

[17] I. Jun, N. Sunwoo, L. Sung, H. Kim, J. Woo, and C.P. Shin, Jpn. J. Appl. Phys. 52. **025003** (2013.)

[18] M. Kawakami, A.B. Hartanto, Y. Nakata, and T. Okada, Jpn J. Appl. Phys. **42**, L33 (2003).

[19] K. Kitamura, T. Yatsui, and M. Ohtsu, Appl. Phys. Express **1**, 081202 (2008).

[20] S. Oh, T. Nagata, J. Volk, and Y. Wakayama, Appl. Phys. Express **095003**, 5 (2012).

[21] S. Park, W. Jung, and C. Park, Jpn. J. Appl. Phys. **025502**, 52 (2013).

[22] Int. Zinc Association, Zinc Recycling (2011)

[23] Y. Hattori, S. Mukasa, H. Toyota, T. Inoue, and S. Nomura, Mater. Chem. Phys. **131**, 425 (2011).

[24] Y. Hattori, S. Nomura, S. Mukasa, H. Toyota, T. Inoue, and T. Kasahara, Journal of Alloys and Compounds **560**, 105 (2013).

[25] Y. Hattori, S. Nomura, S. Mukasa, H. Toyota, T. Inoue, and T. Kasahara, J. Alloys Compd. **560**, 105 (2013).

[26] S. Kubo and M. Nakagawa, Chem. Lett. **41**, 1137 (2012).

[27] S.C. Singh, R.K. Swarnkar, and R. Gopal, **33**, 21 (2010).

[28] P.B. Khoza, M.J. Moloto, and L.M. Sikhwivhilu, J. Nanotech. **2012**, 1 (2012).

[29] S.C. Singh and R. Gopal, Bull. Mater. Sci. **30**, 291 (2007).

[30) A. A. Revina, E. V. Oksentyuk, and A. A. Fenin, Protection of Metals **43**, 554 (2007).

[31] S. Nomura, S. Mukasa, H. Toyota, H. Miyake, H. Yamashita, T. Maehara, A. Kawashima and F. Abe, Plasma Source Sci. Technol. 20 (2011), 034012

[32] T. Maehara, I. Miyamoto, K. Kurokawa, Y. Hashimoto, A. Iwamae, M. Kuramoto, H. Yamashita, S. Mukasa, H. Toyots, S. Nomura and A. Kawahima, Plasma Chem. Plasma Process 28 (2008), pp. 467-482

[33] A. Nomura, H. Toyota, S. Mukasa, Y. Takahashi, T. Maehara, A. Kawashima and H. Yamashita, Appl. Phys. Express 1 (2008), 046002

[34] J. Liao, H. Wu, W. Fu, S. Ci and Q,Chen, Hydrometallurgy 121-124 (2012)

[35] H. . Ebrahim and E. Jamshidi, Trans ChemE, Vol. 79 (2001)

[36] C. Wieckert and A. Steinfield, J. Solar Energy Eng. Vol 124 (2002)

Chapter 5

Alcoholic Solvent Reduction of Zinc Oxide Nanoparticles using Microwave Plasma In-Liquid

5.1 Introduction

The rise in the demand for oil, limitation of non-renewable energy resources as well as the effects of global warming has forced us to consider alternative energy storage and conversion systems. Recently, nanostructured materials have attracted attention for their application in energy storage systems, especially those with desirable charge/discharge rates such as batteries[1][2]. Zinc air battery becomes an attractive option due to its beneficial characteristic, such as high-energy density, low cost, and environmental benignity. However, the formation of large quantity of zinc oxide along with issues arising regarding

its recycling present some problems from a commercial point of view for the development of a rechargeable zinc-air battery under practical condition.

For the synthesis of ZnO quantum particles, nucleation and growth occur rapidly in the presence of longer chain length alcohol[3]. By sonochemical method, H_2PtCl_6 was reduced to Platinum (Pt) nanoparticles when using methanol as solvent, while agglomerated Pt nanoparticles were synthesized when using ethanol[4]. Pt nanoparticles and nanorods were also synthesized by microwave-assisted solvothermal techniques by employing methanol and ethanol as both reducing agents and solvent[5]. The UV pulsed laser irradiation of iron powder in methanol produces a solution of iron oxide nanowires and iron nanoparticles are obtained by using ethanol, isopropanol and glycol[6].

Alcohol has been used as reductant in many kinds of metal nanoparticles synthesis, due to the non-toxic properties and environmental friendly, such as Platinum[4,5], Silver[7,8], Graphene[9], Zinc Oxide[3], [10], Titania[11,12], Iron Oxide[6], and Copper[13] just to name a few. Therefore, by combining alcohols with efficient heating would necessary increasing the reduction reaction in the alcohol processes. In-liquid plasma is suitable for generating a high temperature. Moreover, by applying plasma in alcoholic solvent, the oxidative or reductive

atmosphere of the vapor of the liquid can determined the physical properties of the synthesized nanoparticles.

Zn and zinc nanoparticles are synthesized from zinc electrode by applying plasma in liquid generated by microwave radiation of 250 W[14]. In previous study, a cubic and hexagonal zinc nanoparticles were synthesized by 2.45 GHz microwave in-liquid plasma through reduction of zinc oxide using ethanol as reducing agents. A decreasing of mass ratio of oxygen to zinc was confirmed although some oxide was observed to remain[15]. In order to achieve perfect reduction, the type of solvent and appropriate temperature for reduction should be examined.

In this research, ethanol and methanol are used as the reducing agents and the influence of solvent to the reduction of oxides is determined.

5.2 Experimental Method

The experimental apparatus and methodolgy for generating MW plasma in liquid, primarily conform to previous work with the goal being improved efficiency[15]. A schematic view of the experimental apparatus is shown in figure 5.1. The coaxial electrode fixed to the bottom of reactor vessel is

composed of a copper inner electrode in 10 mm in diameter with hemispherical tip wrapped in a Teflon coating, and a brass outer electrode. At the bottom of the vessel, 60-degree angled polycarbonate from the previous work is replaced with an aluminium plate of 39 mm in diameter with a tiny hole at the center placed above the tip of coaxial electrode. With the addition of plate, the emission of plasma appeared stronger to the naked eye and continued without pause as the gap between the plate and the coaxial electrode is continuously filled with vapor[16]. A copper tube 3 mm in outer diameter and 2 mm in inner diameter used as a counter electrode was placed 1 mm away from the coaxial electrode.

ZnO powder, labeled 200 mesh, 99,999% (NEWMET KOCH) were used. A 0.3 gm of ZnO powder was dissolved in 120 ml both of ethanol and methanol. The mixture was agitated using an ultrasonic device until the powder was dispersed sufficiently. The dispersion was poured into vessel and pressure then decreased into 30 kPa using an aspirator. The liquid was circulated using a gear pump, and coursed from the counter electrode toward the top of inner electrode.

By adjusting a plunger and stub tuner, the input power was adjusted to 400 W until plasma irradiation occured between the coaxial electrode and counter electrode. The plasma emission spectrum was measured using a

spectroscope (PMA-11 HAMAMATSU), while the synthesized materials were identified using energy-dispersive x-ray spectrometry (EDS) as well as by observation using a transmission electron microscope (TEM) (JEM-2100, JEOL).

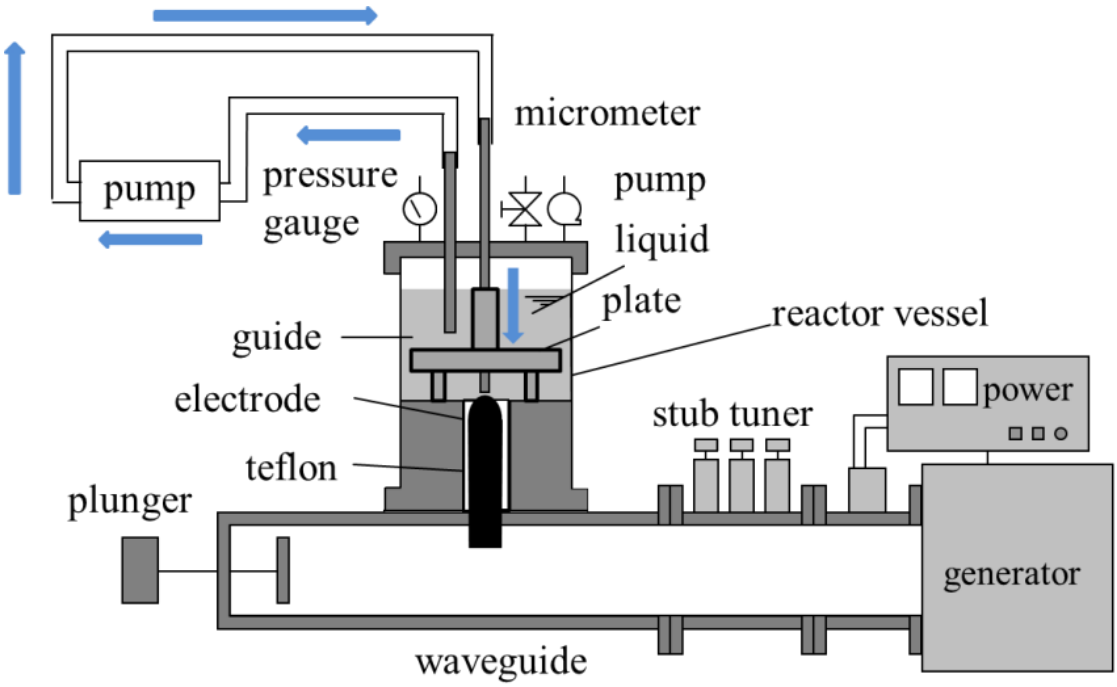

Figure 5.1 Experimental Apparatus

5.3 Result and Discussion

From the calculation of chemical potential of ethanol and methanol, the reduction of ZnO is predicted by consideration of chemical equilibrium. Thermal equilibrium composition of dominant products when zinc oxide reacts with ethanol and methanol was calculated from JANAF Thermodynamical Tables. The Gibbs energy change of zinc oxidation indicates that a reducing environment occurs if the temperature is higher than 1140 K[15]. As shown in figure 5. 2 (a) and 5. 2 (b), at around of temperature 1140 K, the main product become hydrogen and carbon monoxide. A greater proportion of CO is required for oxide reduction. At this temperature, oxide from zinc start to release and bind with CO and H_2, so the production of H_2O and CO_2 increases. At around 1900 K, the mole fraction of CO_2 and H_2O is reduced. Oxide reduction is considered to continuously develop within this range of temperature because mole fraction of O_2 become higher in the same time mole fraction of H_2O and CO_2 decrease.

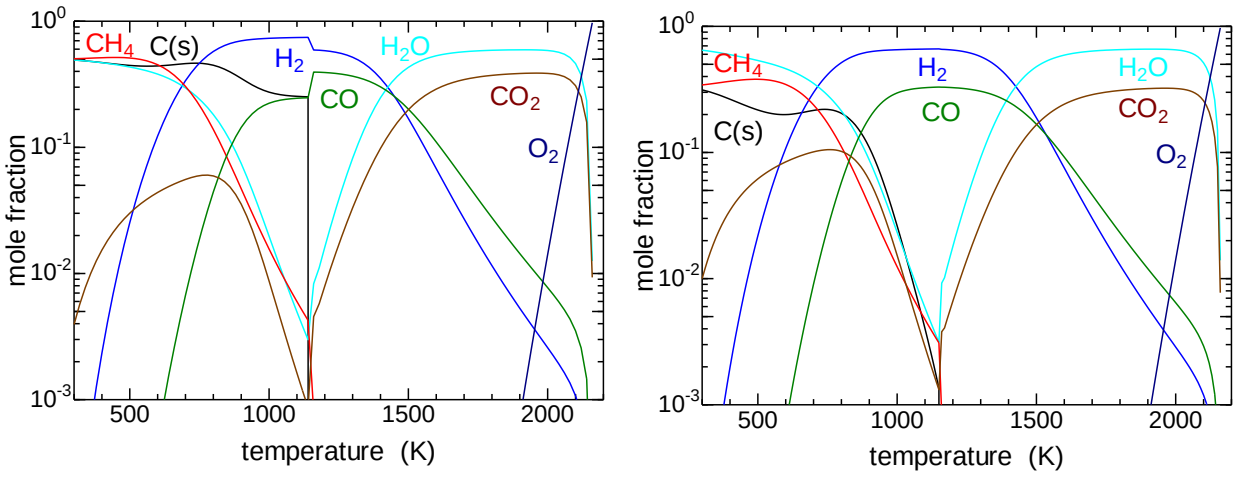

Figure 5.2. Mole fraction of thermal equilibrium (a)ethanol, (b) methanol

Ethanol and Methanol can be an energy source by themselves. The total enthalpy change of these solvents for the reduction of 1 mole ZnO is shown in figure 5. 3. The theoretical entalphy for reduction of ZnO is 348.3 kJ. For ethanol, when the temperature is 1150 K, the entalphy change is 388 kJ which is higher than the theoretical entalphy. Because the dominant contents of the products from ethanol are hydrogen, carbon monoxide and solid carbon, the total entalphy is higher than that of ethanol. When the temperature is between 1500 and 2000 K, the entalphy change becomes less than 348.3 kJ, with the minimum being 144 kJ.

The same tendency is shown when applying methanol as a reducing agent. Entalphy required decreases with a temperature increase until 1400 K with the low entalphy values occuring around 1500 K and 2000 K. It is assumed that a reduction reaction is taking place within these area. Methanol has a lower enthalpy required than ethanol. It is assumed that as the number of carbons in the alcohol increases, the enthalpy needed to reduce oxygen also increases. When alcohol is acting as a reducing agent, some of covalent bonds are broken and new bond formed. More energy is released from the formation of bonds, then absorbed to break the bonds of the alcohol.

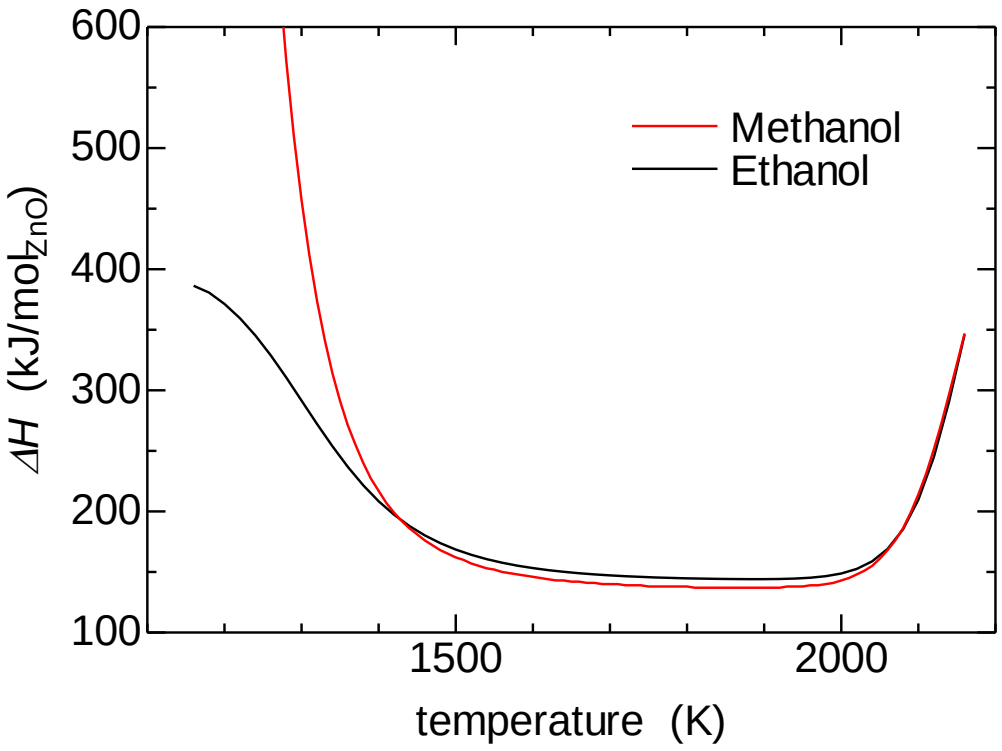

Figure 5.3 Entalphy required due to temperature change

By applying 400 W of input power, plasma was generated about 10 minutes. When ethanol was used, violet plasma emission was observed by the naked eye, when using methanol, violet and blue-white emission was observed. Spectroscopic measurement was employed using PMA-11 C7473 (Hamamatsu) to determine the emission spectrum both for ethanol and methanol. Figure 5. 4 (a) shows the emission spectrum when using ethanol, with characteristic for the zinc line detected at 468.0, 472.2, 481.1, and 636.2 nm. The same peak were

also observed when methanol presented a violet emissions as shown in Figure 5. 4 (b) with an Hα peak occur at 656 nm. The Hα peak, then appears higher in figure 5. 4 (c), which is the reason for the change of plasma emission color from violet into blue-white.

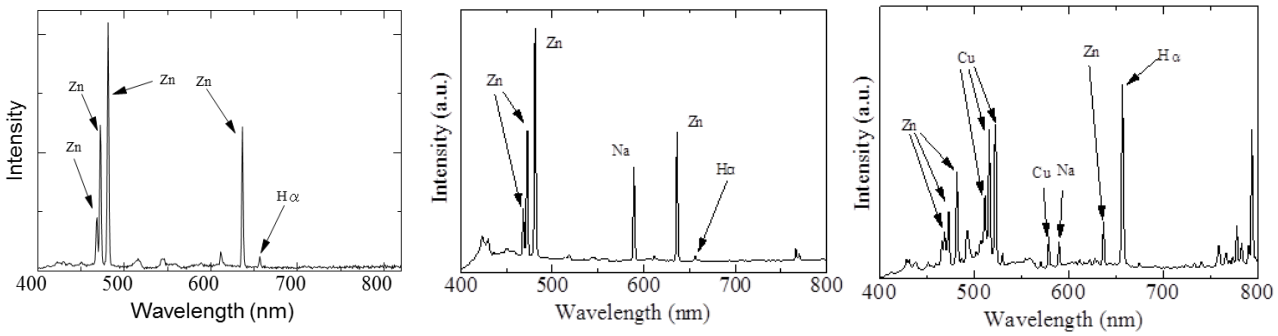

(a) (b) (c)

Figure 5.4 Spectrum of plasma emission (a)ethanol, (b)methanol(violet), (c)methanol(white-blue)

From the theoretical analysis of thermal equilibrium, in order to reduce oxygen, the appropriate temperature are found to be in the range of 1500 to 2000 K. Chao et al. reported that reducing ZnO by silicon is thermodynamically possible at temperature of 1100 to 1500 K[17]. ZnO reduction using CO shows a strong temperature dependence within the 1183 to 1497 K temperature range[18]. A spectrum simulation program was applied to calculate the spectral

line at various temperatures as well as for comparison with spectrum obtained from the experiment. Figure 5.5 shows CO spectral band were observed by plasma emission at 250 nm to 350 nm. The rotational and vibration temperature can be attained by matching the configuration of the spectral band to that of the computational simulation. There is a close match with the measured value at 1600 K. Since this temperature is within the range as the theoretical result, it is believed that plasma in liquid provides a reducing environment for oxide.

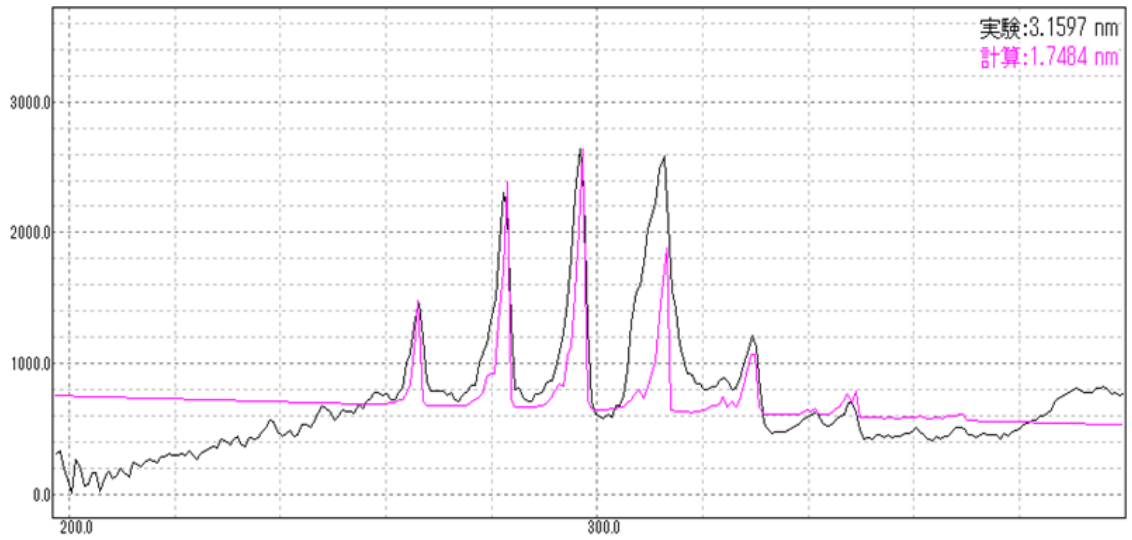

Figure 5.5 Comparison of the experimental CO spectral band
and the temperature calculated by computational simulation.
The red line in the figure is the spectrum chart attained from simulation

After plasma irradiation, the produced nanoparticle was examined by transmission electron microscope (TEM, 200 KV, JEOL, JEM-2100). The ZnO nanoparticles used throughout this study were a mixture of rectangular and hexagonal of 50 to 200 nm in length before plama irradiation[15]. Change of nanoparticle shape was not confirmed after plasma irradiation either in ethanol and methanol as shown in figure 5 .6. 100 nm of rectangular particles were observed both in ethanol and methanol and particle aggregation was remarkable in the remaining liquid of methanol. However, the agglomeration phenomena has not been confirmed yet.

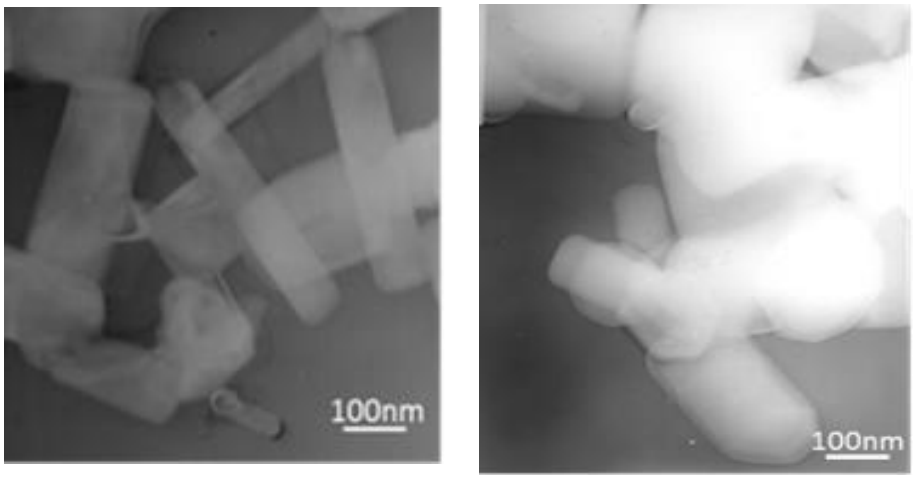

(a) (b)

Figure 5.6 TEM image of nanoparticle obtained
(a) in ethanol, (b) in methanol

Despite the lack of significant difference of particle synthesized after plasma irradiation, hardly any oxygen is detected in comparison to the amount before plasma irradiation. From energy dispersive x-ray spectrometry (EDS) results, the mass ratio of oxygen to zinc was reduced from 24% before plasma irradiation in figure 5. 7(a), to 6% after plasma irradiation in ethanol as shown in figure 5. 7(b) and 0.46% in methanol as shown in figure 5. 7(c).

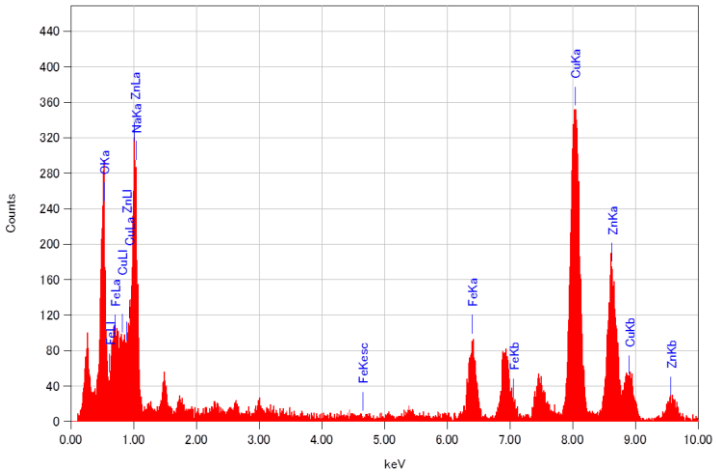

(a)

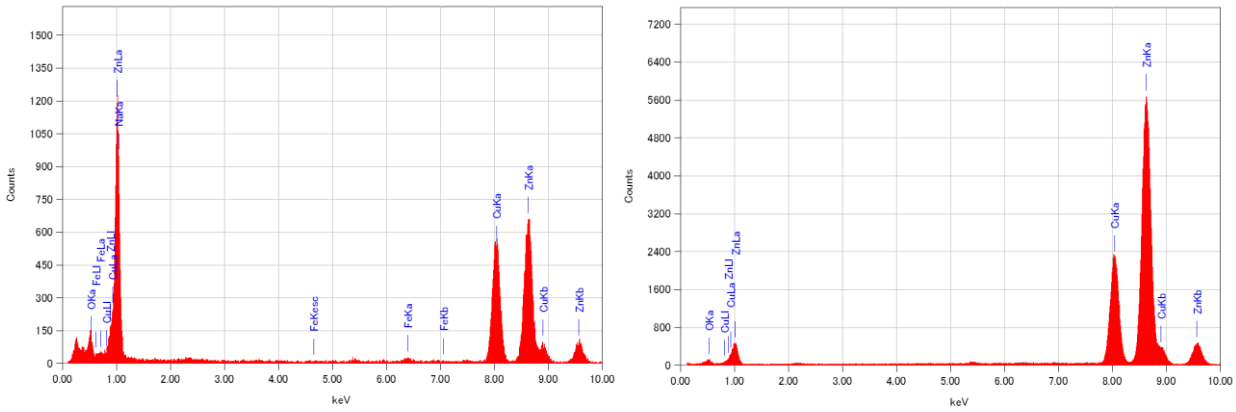

(b) (c)

Figure 5.7 EDS spectra of liquid obtained (a)before plasma irradiation, (b) after plasma irradiation in ethanol, (c) in methanol

Several reports have been written on the recovery of zinc. However, there is no information yet about its recovery in nanoparticles size. By using carbon in the presence of various additives, zinc product is gaseous and oxygen gases tends to recombine resulting in the formation of ZnO which further decreases the recovery efficiency[19][20]. By using methane as reducing agents to recover zinc, the product is also in a gas form and needs to be cooled down quickly to separate it from the syngas[20,21]. Nanoparticles produced by in-liquid plasma method are dispersed in the remaining liquid. By evaporating the liquid, nanoparticles can be easily collected. Additionally, since the reaction area is separated from the air, re-oxidation is avoided.

5.4 Conclusion

Zinc nanoparticles have been synthesized from reduction of zinc oxide nanoparticles using both ethanol and methanol while applying microwave plasma in-liquid. In this method, reduction takes place in the range temperature of 1500 to 2000 K. Change of nanoparticles shape was not confirmed after plasma irradiation. However, the mass ratio of oxygen to zinc was decreased both in ethanol and methanol from 24% to 6% and 0.46% respectively. Agglomerated particles were observed when using methanol, though the entalphy required for reduction is lower than that of ethanol. It is assumed that agglomerated phenomena have a close relationship with entalphy. These results therefore open up promising avenues for reduction in nanoparticle size. Despite the possibility of oxide reduction offered by in-liquid plasma method, it is necessary to carry out further investigations to determine the optimal reaction parameter and reduction mechanism.

References

[1] J.-S. Lee, S. Tai Kim, R. Cao, N.-S. Choi, M. Liu, K. T. Lee, and J. Cho, "Metal–Air Batteries with High Energy Density: Li–Air versus Zn–Air," *Advanced Energy Materials*, vol. 1, no. 1, pp. 34–50, Jan. 2011.

[2] V. Caramia and B. Bozzini, "Materials science aspects of zinc–air batteries: a review," *Materials for Renewable and Sustainable Energy*, vol. 3, no. 2, p. 28, Apr. 2014.

[3] Z. Hu, G. Oskam, and P. C. Searson, "Influence of solvent on the growth of ZnO nanoparticles," *Journal of Colloid and Interface Science*, vol. 263, no. 2, pp. 454–460, Jul. 2003.

[4] L. Obreja, N. Foca, M. . Popa, and V. Melnig, "Alcoholic Reduction Platinum Nanoparticles Synthesis by Sonochemical Method," *Biomaterials in Biophysics, Medical Physic and Ecology*, no. 11, 2008.

[5] D. Li and S. Komarneni, "Synthesis of Pt Nanoparticles and Nanorods by Microwave-assisted Solvothermal Technique," vol. 5, pp. 1566–1572, 2006.

[6] S. Mollaha, C. E. G. S. J. Henleyb, and S. R. P. Silvab, "Photo-Chemical Synthesis of Iron Oxide Nanowires Induced by Pulsed Laser Ablation of Iron Powder in Liquid Media," *Integrated Ferroelectrics : An International Journal*, vol. 119, no. 1, pp. 45–54, 2010.

[7] D. O. Oseguera-Galindo, a. Martínez-Benítez, a. Chávez-Chávez, G. Gómez-Rosas, a. Pérez-Centeno, and M. a. Santana-Aranda, "Effects of the confining solvent on the size distribution of silver NPs by laser ablation," *Journal of Nanoparticle Research*, vol. 14, no. 9, p. 1133, Aug. 2012.

[8] H. Hah, S. M. Koo, and S. H. Lee, "Preparation of Silver Nanoparticles through Alcohol Reduction with Organoalkoxysilanes," pp. 467–471, 2003.

[9] C. Gong, M. Acik, R. M. Abolfath, Y. Chabal, and K. Cho, "Graphitization of Graphene Oxide with Ethanol during Thermal Reduction," *The journal of Physical Chemistry C*, vol. 116, no. 18, pp. 9969–9979, 2012.

[10] P. Banerjee, S. Chakrabarti, S. Maitra, and B. K. Dutta, "Zinc oxide nano-particles--sonochemical synthesis, characterization and application for photo-remediation of heavy metal.," *Ultrasonics sonochemistry*, vol. 19, no. 1, pp. 85–93, Jan. 2012.

[11] B. Liu, Y. Wang, Y. Huang, P. Dong, and S. Yin, "Morphological Control and Photocatalytic Activities of Nitrogen-doped Titania Nanoparticles by Microwave- assisted Solvothermal Process," vol. 48, pp. 249–252, 2012.

[12] D. Liang, C. Cui, H. Hu, Y. Wang, S. Xu, B. Ying, P. Li, B. Lu, and H. Shen, "One-step hydrothermal synthesis of anatase TiO2/reduced graphene oxide nanocomposites with enhanced photocatalytic activity," *Journal of Alloys and Compounds*, vol. 582, pp. 236–240, Jan. 2014.

[13] T. Nakamura, Y. Tsukahara, T. Sakata, H. Mori, Y. Kanbe, H. Bessho, and Y. Wada, "Preparation of Monodispersed Cu Nanoparticles by Microwave-Assisted Alcohol Reduction," *Bulletin of the Chemical Society of Japan*, vol. 80, no. 1, pp. 224–232, 2007.

[14] Y. Hattori, S. Mukasa, H. Toyota, T. Inoue, and S. Nomura, "Synthesis of zinc and zinc oxide nanoparticles from zinc electrode using plasma in liquid," *Materials Letters*, vol. 65, no. 2, pp. 188–190, Jan. 2011.

[15] N. Amaliyah, S. Mukasa, S. Nomura, and H. Toyota, "Plasma In-liquid Method for Reduction of Zinc Oxide in Zinc Nanoparticle Synthesis," *Material Research Express*, vol. 2, no. 2, 2015.

[16] Y. Hattori, S. Nomura, S. Mukasa, H. Toyota, T. Inoue, and T. Kasahara, "Synthesis of tungsten trioxide nanoparticles by microwave plasma in

liquid and analysis of physical properties," *Journal of Alloys and Compounds*, vol. 560, pp. 105–110, May 2013.

[17] C. Qi-yuan, "Thermodynamic Analysis of Silicothermic Reduction Zinc Oxide in Vacuum," *Acta Phys.-Chim. Sin.*, vol. 27, no. 6, pp. 1312–1318, 2011.

[18] S. Jordens and S. Escobedo, "Dependence of zinc oxide reduction rate on the CO concentration in CO / CO2 mixtures," *Thermochimia Acta*, vol. 278, pp. 129–134, 1996.

[19] B.-S. Kim, J.-M. Yoo, J.-T. Park, and J.-C. Lee, "A Kinetic Study of the Carbothermic Reduction of Zinc Oxide with Various Additives," *Materials Transactions*, vol. 47, no. 9, pp. 2421–2426, 2006.

[20] C. Wieckert and A. Steinfeld, "Solar Thermal Reduction of ZnO Using CH4:ZnO and C:ZnO Molar Ratios Less Than 1," *Journal of Solar Energy Engineering*, vol. 124, no. 1, p. 55, 2002.

[21] H. A. Ebrahim and E. Jamshidi, "Kinetic Study of Zinc Oxide Reduction by Methane," *TransIChemE*, vol. 79, no. January, 2001.

Chapter 6

General Conclusion

As energy sources tend to be increasingly shorter, especially for electricity supply, it is necessary to develop an energy storage technology showing high energy efficiency, low cost, environmentally benign, as well as safety and realibility.

Among others metal used in metal-air battery system, zinc has the lowest equivalent weight, the lowest ecological concern, and a very attractive cell voltage in conjunction with an oxygen electrode. The zinc-air battery system can therefore be regarded as a sustainable and very promising power source.

The main factor which has restricted the appeal of Electric Vehicles is their limited range. The range is governed by how much electrical energy the battery can store and the weight of battery. Therefore the most important performance metric

for EV batteries is the amount of energy the battery can store per unit weight. This is called its specific energy and is measured in Watt-hour per kilogram (Wh/kg). The zinc-air battery, however, has the highest specific energy of all.

There are other factors that have to be taken into account, but the zinc-air technology has long been recognized as attractive for this reason. Zinc air has such high specific energy because one of the reactants is external to the battery – the oxygen in the air. Therefore the vehicle does not have to carry that material on the board in the battery, greatly reducing the weight.

However, in the zinc-air battery, a combination of high-energy density with atmospheric oxygen will lead to the formation of zinc oxide in large quantity.

Plasma in-liquid method is proposed as a method of recycling air batteries by reduction of zinc oxide. Microwave-induced plasma is generated in alcoholic solvents as a reducing agent in which zinc oxide is dispersed.

A cubic and hexagonal shapes of zinc nanoparticles are synthesized from reduction of zinc oxide powder which ethanol act as a reducing agents in chapter 4. Zinc nanoparticles of about 30 to 200 nm along with fiber flocculates 10 nm in

diameter are found at the tip of electrode and in the remaining liquid after plasma generation. Absorption spectroscopy confirm that during plasma irradiation, there is a great reduction as the absorbance decrease which The Beer–Lambert law predicts that the intensity of the absorption peak is directly proportional to the concentration of the compound.

From the chemical equilibrium calculation, it is also confirmed that all temperatures in plasma shown above exceed 1140 K, therefore the reaction field provided by in–liquid plasma is a reducing atmosphere for zinc oxide.

Influence of solvent used for reducing zinc oxide is investigated in chapter 5. By applying 400 W of microwave generator input power, the total enthalpy change is determined. Enthalpy required decreases with a temperature increase until 1400 K with lower entropy value occurring around 1500 K and 2000 K. It is assumed that both when using ethanol and methanol a reduction reaction is taking place within this area. However methanol has a lower enthalpy required than ethanol.

Despite of no change of nanoparticle shape is confirmed after plasma irradiation either in ethanol and methanol, hardly any oxygen is detected in comparison to the amount

before plasma irradiation. From energy dispersive x-ray spectrometry (EDS) results, the mass ratio of oxygen to zinc was reduced from 24% before plasma irradiation to 6% after plasma irradiation in ethanol and 0.46% in methanol.

This dissertation work has shown that in-liquid plasma method is feasible for reduction of zinc oxide in order to recycling zinc-air batteries. The present method provides a preventing from re-oxidation because the reaction area is separated from the air by the liquid. An additional advantages to this method is the easy collection of the product since the reduced metal remains in the liquid as dispersed material. The results are open up promising avenues for reduction in nanoparticle size.

Acknowledgement

The present dissertation has been achieved in the Doctoral program of Graduate School of Science and Engineering, Ehime University, Japan.

This dissertation would have not here without the help, support, guidance and efforts of a lot of people. At this point, I would like to express my sincere gratitude to all those who have enabled me to complete this research.

First and foremost, I would like to express the deepest appreciation to my advisor, Professor Shinfuku Nomura, for all the wisdom, encouragement, guidance, and invaluable suggestion during my study. For the unwavering support, I am truly grateful to have him as my professor.

My sincere thanks also go to all dissertation advisers, Professor Hiromichi Toyota and Associate Professor Masaya Nakahara for their encouragement and support.

I am deeply grateful to Senior Assistant Professor Shinobu Mukasa for providing enormous amounts of invaluable response for this dissertation.

During the course of this work, the constant association with the members of nanoparticle team has been most pleasurable. I would like to thank Mr. Kiniyuki Gangi, Mr. Tomohide Kitamae, Mr. Nobuyuki Doi, Mr. Yuya Sumoto and Mr. Yuki Udaka. I also would like to thank Dr. Erwin Eka Putra for introducing me to this laboratory for the first time and supporting me to take this change, Dr. Yoshiaki Hattori for some discussion regarding this study and usage of some apparatus, Mr. Atsushi Ito as my first tutor, Mr. Toshimitsu Tamura and all members (past and present) in Heat and Mass Transfer Laboratory for helpful assistance. Next I thank to all doctoral students in Heat and Mass Transfer Laboratory Mr. Fadhli Bin Syahrial, Mr. Muhammad Agung, and Mr. Andi Amijoyo Mochtar for their great support.

I would like to acknowledge the financial support from Directorate General of Human Resources for Science, Technology and Higher Education of Indonesia. I would also like to thank the Graduate School of Science and Engineering Ehime University for its financial funding for attending the conference.

I would like to thank my mother, my father and all of my family in Indonesia for their infinite support. I also heartily thank my son Muhammad

Faiz Al-Ghifari, my daughters Nayla Syafiqah and Muthia Raihanun for all their love, understanding and patience.

Finally, this last word of acknowledgement I have saved for my dear husband Ismail Rahim. Thank you for being the best partner during my study, for being with me through the good and bad times, for all your love and support. To you I am eternally grateful.